nature portfolio

Peer Review File

A Metamaterial Scaffold Beyond Modulus Limits: Enhanced Osteogenesis and Angiogenesis of Critical Bone Defects

Corresponding Author: Professor Yufeng Zheng

Parts of this Peer Review File have been redacted as indicated to remove third-party material.

This file contains all reviewer reports in order by version, followed by all author rebuttals in order by version.

A version of this paper was originally rejected for publication by Nature Communications, however that decision was reconsidered after appeal by the authors.

Version 1:

Reviewer comments:

Reviewer #1

(Remarks to the Author)
The manuscript introduces a strategy for bone regeneration through the use of a two-stage metamaterial scaffold (TMS). The authors conduct extensive mechanical design and testing. In vivo implantation studies that provide substantial data on osteogenesis and mechanistic insights into the TMS's bone-promoting properties. The TMS design resolves the key strength limitation of low-modulus scaffolds, And potentially offers a significant protocol for exploring the biomechanics of osteogenesis. Overall, this is an interesting and novel study that intrinsically combines the concept of mechanical metamaterial with the mechanics of bone regeneration. I recommend this article for publication in Nature Communications after minor revisions to improve clarity and accessibility to a wider audience.

1. The author mentioned in the Discussion that TMS was used for compression-dominant bone implants. Due to the radius bone and wrist joints, TMS in the ulna treatment can avoid excessive bending or torsion. Meanwhile, the results successfully demonstrated its effectiveness in reconstructing critical ulnar defects, what are the possibility of applying TMS in other bone implant sites? And also, the flexibility of TMS design to fit other shape of bone implant sites? This should be discussed in more detail.
2. The subplots order of Fig 3 and Fig 4 is inconsistent, including the bar charts. The results of the control groups should be presented first, followed by the TMS results.
3. Fig. 4i contains two meaningless letters, "e".
4. The Western Blot data in Fig 5e should not be separated to ensure scientific accuracy; it can be replaced with Fig. S14e.
5. An incorrect reference to Fig. S4a in Supplementary Note 4. It should be Fig.S5.

Reviewer #2

(Remarks to the Author)
The study investigates the application of meta-structured scaffolds and a two-stage deformation process to enhance osteogenesis and angiogenesis. The authors conducted static and dynamic mechanical tests, along with in vivo experiments, to evaluate bone regeneration. While the study addresses an important research area, the manuscript contains several critical issues that need to be addressed to improve its scientific rigor and overall quality.
1. The introduction of the study lacks a coherent flow and does not effectively highlight the key points of the topic. For instance, the first paragraph attempts to emphasize the importance of scaffolds, followed by statistical details from published studies, and then shifts to metamaterials without clear connections. The authors need to reorganize the introduction section to clearly outline the problem and the rationale for the study. Additionally, Fig. 1 inadequately depicts the workflow, with poorly aligned components and inconsistent sizes, and requires revision for clarity.
2. The mechanical design of the TMS and CS scaffolds is unclear. Specifically, the TMS design's connection points and the rationale behind the inclusion of additional spring structures are insufficiently justified. Within the TMS structure, the two springs are connected only at a single point in the middle. If lg=0, the springs should theoretically connect along their entire

length, not just at one point. Furthermore, the authors stated that dp=0 was used to create a control group, yet they previously described the addition of pillars to connect the springs. If the pillars can be removed, it raises the question of why the straight lines were designed in the first place.
3. In the sentence, “The CS displayed a stress-strain curve in compression that closely resembled that of typical bone implants (Fig. 2b)”, the authors claim that CS scaffolds resemble typical bone implants, citing a reference (below) to support this assertion. The cited reference does not provide relevant stress-strain data, and the authors should instead compare their findings with the stress-strain properties of natural bone for a scientifically valid comparison.
- Reference: Z. Jia, X. Xu, D. Zhu, Y. Zheng, Design, printing, and engineering of regenerative biomaterials for personalized bone healthcare. Progress in Materials Science. 134, 101072, (2023)
4. Based on Figs. 2b and 2c, these figures should correspond to TMS and CS, respectively. However, in Fig. 2d, the colors and behaviors differ from those in the earlier figures, creating inconsistency. More critically, a small toe region is observable in Fig. 2b but is absent in Fig. 2d, raising concerns about the accuracy of the results. Interestingly, this small toe region reappears in Fig. 2e, further complicating the interpretation. If CS exhibits a toe region with two-stage deformation, what then differentiates CS from TMS? Additionally, why was the CS2 configuration not shown separately for clarity and comparison?
5. Based on the following paragraph in the manuscript, how did the authors confirm osteogenesis? Detailed justification and evidence are required to support these claims.
- “The TMS demonstrates an effective modulus of only 13.4 MPa, producing an inflection point strain of 2.5% with a small force of 10 N. Additional compressive forces result in the stiff stage of the TMS, where the modulus reaches 318 MPa. When subjected to a total force of 60 N (twice the animal's body weight), the strain is still within 5%, thus ensuring both strength and osteogenesis”.
6. The three-point bending test in Fig. S3 includes additional parts to control movement, which could affect scaffold properties. The rationale behind these design choices and their alignment with standard protocols should be clarified.
7. According to the paragraph, "However, the TMS has a decreasing fatigue damage strain, which indicates that the TMS has a certain work hardening effect during fatigue tests. Both compression unloading and fatigue tests demonstrated the resilience of TMS. In short, the TMS exhibits tunable, two-stage compression behavior and maintains resilience well under fatigue loading," the authors suggest that TMS has superior fatigue properties compared to CS. However, based on the strain values presented in Fig. 2, CS exhibits lower deformation after 80,000 cycles, implying that CS may demonstrate better long-term durability. This apparent contradiction raises questions about the interpretation of the fatigue test results and the potential for earlier failure of TMS under similar fatigue conditions.
8. In the sentences, "The geometry differences among CS, CS2, and TMS are the small gap (lg) and pillar (dp) as mentioned before. Thus, except for the mechanical properties, the impact of other geometry factors on osteogenesis, such as pore size [20, 21], curvature [22, 23], and porosity [9], can be neglected," the authors dismiss the influence of key geometric factors on osteogenesis. However, the geometry differences, such as variations up to 0.25 mm, are substantial enough to significantly affect mechanical properties. It is therefore scientifically inconsistent to assume that these changes have negligible effects on osteogenesis.
9. The differences between CS and TMS in Fig. S7 are not clearly discernible at the current resolution. To effectively highlight these distinctions, higher-magnification imaging should be employed.
10. In TMS structures, a small lg creates small pores in the scaffolds, which could influence the bone healing process. In contrast, the larger pore size in CS structures may lack the same potential to accelerate bone regeneration, as shown in Figs. 3 and 4. Additionally, these differences, along with variations in porosity, could impact the modulus of the newly formed bone due to the stress shielding effect. To comprehensively evaluate the TMS and CS structures, it is essential to consider all relevant variables, including pore size, porosity, and their potential biological and mechanical impacts.
11. In the discussion section, finite element modeling (FEM) was utilized to simulate the strain behavior of bone tissue during osteogenesis. However, in the "Mechanical Tests and Simulations" section, the focus is primarily on the mechanical properties of the main scaffolds. According to Fig. 6, the simulation incorporates both the scaffolds and bone tissue, using the mechanical properties of the callus to represent bone tissue during early osteogenesis (as described in "Tissue Strain Analysis").
This raises several important questions:
- Why were the specific mechanical properties of the callus chosen for the simulation?
- Did the authors account for the interaction between the scaffolds and host tissue in their modeling approach?
- Most critically, the study did not validate the FEM results with experimental data, which is essential to confirm the accuracy and reliability of the simulations.
Addressing these points would greatly enhance the scientific rigor and reliability of the findings.
12. One major concern in the present study is the quality and resolution of the 3D printing process, which was not adequately addressed in the results or discussion. Poor printing quality can significantly impact the structural integrity and performance of the scaffolds, potentially compromising the reliability of the results. To evaluate the printing accuracy, SEM images of the fabricated scaffolds should be compared with the designed models. Additionally, Fig. S1 reveals indications of low printing quality, which further emphasizes the need for a detailed assessment of the manufacturing process and its implications on the study’s findings.
13. In the "Mechanical Tests and Simulations" section, the authors did not adhere to a standard protocol for calculating the mechanical properties of the scaffolds or for evaluating the non-porous materials used in the FEM simulations. This lack of standardization raises concerns about the reliability, consistency, and comparability of the mechanical property data and its subsequent use in FEM modeling.

Reviewer #3

(Remarks to the Author)
I co-reviewed this manuscript with one of the reviewers who provided the listed reports. This is part of the Nature

Communications initiative to facilitate training in peer review and to provide appropriate recognition for Early Career Researchers who co-review manuscripts.

Reviewer #4

(Remarks to the Author)
The paper is well researched and the concept is very novel and timely. Although several papers have published on metamaterials, 3D printed bone implants and both combined, the idea of a metamaterial with different properties over different mechanical regimes is very well developed in this paper. The figures are all well-presented and very well organized and detailed. I suggest a number of minor corrections before the paper can be accepted for publication. There are some sections in the introduction that need a bit of rewriting, in particular including more detail on referenced work to provide a clearer picture of the current state-of-the-art in the field. Some parts of the materials and methods section need more detail, both to understand the presented data better and to allow researchers to replicate the body of work. Also in the results there are a few sections that need more clarification and corrections.

These points are highlighted in more detail below:

Introduction

• Line 40-41 “modulus of metal” is too vague considering how many metals there are. Be more specific in defining the metals used for bone implants and how it relates to bone tissue engineering.
• 47-48 “optimised osteogenesis” in terms of what, osteoblast proliferation, callus formation. The finding is not necessarily because of the callus formation, that is simply an observation.
• 49 reconstruction may be the wrong word given it indicates human intervention rather than on its own healing
• In general the references in the main body of text accurately describe whats happening in the text but may need more explanation of exactly why they were used.
• Some of the English reads poorly. For example in lines 58-59, the use of “specially architectured” and “properties beyond” are not especially descriptive and require revision.
• 60-61 should explain exactly why specific geometries are non-conducive to osteogenesis, in order to better set up why the proposed design is more effective according to the study.
• “The TMS exhibits a robust capacity to promote bone reconstruction compared to two classic scaffolds (CS with modulus of 500 MPa, CS2 with modulus of 13 MPa)”, SHOULD READ “The TMS exhibits a robust capacity to promote bone reconstruction compared to two classic scaffolds with moduli of 500 MPa (CS) and 13 MPa (CS2) respectively.”
• Although this body of work can be considered novel it is worth mentioning some of the fabrication, characterisation and testing of metamaterial based bone tissue engineering scaffolds, as data does exist out there outside of the referenced papers in the study.

Materials and Methods Section

As a general rule in all the materials and methods the amount of technical and biological replicates needs to be provided (n=? N=?). There are some references to repeats in the main text but this should also be provided in the methods section for clarity.
• Materials and Additive Manufacturing- more detail needed in terms of printing parameters. This includes the beam current, scan speed, linear energy, cooling speed and the slicing layer height.
• Mechanical tests and simulations- there needs to be a mention of the type, model and force rating of the load cell used in this experiment. Consider in the future performing the mechanical testing at the intended operation temperature instead of ambient.
• Animal model establishment- Lines 376 and 377 mention the generation of a defect but how was this defect produced. Line 381 should read “the rest of”
• Radiographic analysis- software should be cited in-text. There should be a description exactly what value Hounsfield units denotes both bone, soft tissue and the implant.
• Nanoindentation- other parameters that need to be described are the displacement, displacement rate and the distance between each indentation for single samples.
• 2nd harmonic generation imaging- the number of measurements taken per image and the number of images used is required.
• Western blot and proteomics analysis. Much more detail in terms of parameters, timings etc for both of these methods. Good examples of methods sections demonstrating the level of detail (https://doi.org/10.1186/s13036-021-00273-6, https://doi.org/10.1016/j.bone.2011.09.039 and https://doi.org/10.1038/s41598-020-75527-2). Please note I do not ask these references to be added to the manuscript they are just examples of detailed methods sections.

Results section

• 87-88 “The TMS, however, exhibits its distinctive two-stage behavior.” explain using the collected data exactly what the behaviour is.
• 92-93 in your materials and methods you mention that 60 N is twice the weight of the average rabbit. However, previously you describe the primary stress conditions as 1/6th of the weight of a rabbit. 1/6th of 30 N is 5 N instead of 10 N (10 N would be 1/3rd of the rabbits weight). Please clarify which is correct, also correct the results and conclusion section accordingly.
• The graphical and data visualisations are of excellent quality. Please add the technical and biological replicates in the figure captions of all figures.

• An exception to this is in figure 4r and 4s. first there is no scale bar in figure 4r and there is no mention of what the size of the scale bar is in figure 4s. In the description of these figures the authors state “the collagen fiber appeared to be more random of CS. Whereas in the TMS, the collagen showed a pronounced orientation parallel to the loads.” (line 222-223). This is not overly clear from the figures and more detail need to be given to support this statement. I can see from the orientation map there seems to be some improvement in orientation, but would it be possible to quantify this a bit more. For example, the authors can measure collagen alignment in the figures via the method given in this paper doi: 10.1007/978-1-4939-7113-8_28), which will provide a stronger argument for this observation.
• Line 237: “Subsequently, proteomic and Western Blotting (WB) were conducted” should be “Subsequently, proteomic analysis and Western Blotting (WB) were conducted”
• While you have correctly noted where there are areas of significant differences between samples, potential reasons must be given for where no significant differences were noted, which in the case of figure 3 appears to be between CS and TMS at 8 weeks (figure 3b), between any group at 8 weeks (3c) and between any groups (figure 3d).
• Figure 5 is excellent, although figure 5f looks more like a graphical abstract or a figure that can be included in the intro to provide a pictorial overview of this study.
• Line 338: “for compress-dominated applications” should be “for compression-dominated applications”

Reviewer #5

(Remarks to the Author)
I co-reviewed this manuscript with one of the reviewers who provided the listed reports. This is part of the Nature Communications initiative to facilitate training in peer review and to provide appropriate recognition for Early Career Researchers who co-review manuscripts.

Version 2:

Reviewer comments:

Reviewer #1

(Remarks to the Author)
The authors well address previous concerns. It deserve a rapid publication in NC.

Reviewer #2

(Remarks to the Author)
The authors have successfully addressed all the reviewer comments, improving the overall quality of the paper. I am pleased to recommend its acceptance.

Reviewer #3

(Remarks to the Author)
I co-reviewed this manuscript with one of the reviewers who provided the listed reports. This is part of the Nature Communications initiative to facilitate training in peer review and to provide appropriate recognition for Early Career Researchers who co-review manuscripts.

Reviewer #4

(Remarks to the Author)
The corrections have addressed my comments and I am happy for the manuscript to be published without any further corrections.

Reviewer #5

(Remarks to the Author)
I co-reviewed this manuscript with one of the reviewers who provided the listed reports. This is part of the Nature Communications initiative to facilitate training in peer review and to provide appropriate recognition for Early Career Researchers who co-review manuscripts.

Response to the Reviewers' Report

We would like to cordially thank the reviewers for the valuable suggestions and comments on our paper. Our response is structured as follows. The original comments from the reviewers are copied below in *blue and italic font*. For each comment, we present a detailed response (black font), a complete description of all the additional experiments and simulations we conducted, and the corresponding manuscript modifications (red font). In the manuscript, the amended parts are shown in red font.

Reviewer #1 (Remarks to the Author):

The manuscript introduces a strategy for bone regeneration through the use of a two-stage metamaterial scaffold (TMS). The authors conduct extensive mechanical design and testing. In vivo implantation studies that provide substantial data on osteogenesis and mechanistic insights into the TMS's bone-promoting properties. The TMS design resolves the key strength limitation of low-modulus scaffolds, And potentially offers a significant protocol for exploring the biomechanics of osteogenesis. Overall, this is an interesting and novel study that intrinsically combines the concept of mechanical metamaterial with the mechanics of bone regeneration. I recommend this article for publication in Nature Communications after minor revisions to improve clarity and accessibility to a wider audience.

Response: We are most grateful for your expressed interest and important comments on this work, which were of great value in improving the scientific quality of this work.

1. The author mentioned in the Discussion that TMS was used for compression-dominant bone implants. Due to the radius bone and wrist joints, TMS in the ulna treatment can avoid excessive bending or torsion. Meanwhile, the results successfully demonstrated its effectiveness in reconstructing critical ulnar defects, what are the possibility of applying TMS in other bone implant sites? And also, the flexibility of TMS design to fit other shape of bone implant sites? This should be discussed in more detail.

Response:

We thank you for the valuable comment. TMS is an innovative metamaterial structure with inherent limitations in its application scope. Specifically, the TMS structure is suitable for bearing compressive forces and is not designed to withstand tensile or torsional forces. Our study aims to explore whether this TMS structure exhibits superior osteogenic effects under compressive loads compared to traditional structures.

Notably, for most bone defect sites (e.g., limbs, spine), the primary force is compressive, as the primary function of bones is to support body weight. While the current TMS design is in the shape of a cylinder, it can be adapted to support bone defects of various applications. This is because the most important property of bone substitutes is to provide adequate support. And cylindrical designs are commonly used for bone substitutes in clinical applications [r1-r3].

In this study, the core innovation of TMS lies in breaking through the limitations of existing scaffold designs in balancing elastic modulus and strength. By introducing a two-stage deformation behavior, TMS simultaneously meets the strength requirements of implants and provides the optimal strain magnitude for osteogenesis. This concept is inherently independent of shape or loading direction. In the future, shape compatibility can be achieved by adjusting the shape of the TMS springs (e.g.,

polygons, ellipses). Additionally, two-stage deformation in the tensile direction can be realized by incorporating limit elongation gaps within the TMS structure. We have included this discussion in the revised manuscript.

[r1] H. Zhou, S. Liu, Z. Li, X. Liu, L. Dang, Y. Li, Z. Li, P. Hu, B. Wang, F. Wei, Z. Liu, 3D-printed vertebral body for anterior spinal reconstruction in patients with thoracolumbar spinal tumors, J Neurosurg Spine (2022) 1-9.
[r2] G. Hou, B. Liu, Y. Tian, Z. Liu, F. Zhou, Reconstruction of Ipsilateral Femoral and Tibial Bone Defect by 3D Printed Porous Scaffold Without Bone Graft: A Case Report, JBJS Case Connect 12(1) (2022).
[r3] G. Hou, B. Liu, Y. Tian, Z. Liu, F. Zhou, H. Ji, Z. Zhang, Y. Guo, Y. Lv, Z. Yang, P. Wen, Y. Zheng, Y. Cheng, An innovative strategy to treat large metaphyseal segmental femoral bone defect using customized design and 3D printed micro-porous prosthesis: a prospective clinical study, J Mater Sci Mater Med 31(8) (2020) 66.

Modification:

While TMS exhibits promising performance in the ulna defects, there is a potential risk that it may only demonstrate the ductile stage behavior when subjected to tensile forces. Consequently, TMS may be more suitable for compression-dominated applications, such as interbody fusion devices. Still, compared with conventional scaffold design strategies of matching modulus to the bone, TMS opens a new scaffold design paradigm of generating sufficient strain of bone tissue to stimulate the regeneration. Above all, such concept can be applied to various materials, and is inherently independent of shape or loading direction. In the future, shape variations can be achieved by adjusting the shape of the TMS springs (e.g., polygons, ellipses). Moreover, two-stage deformation in other loading directions can be achieved by incorporating limit gaps, analogous to the compressive gap in TMS. The protocol of TMS transcends material-specific limitations and can be readily manufactured utilizing commercial 3D printing equipment, underscoring its versatility and accessibility within the fields of biomedical engineering.

2. The subplots order of Fig 3 and Fig 4 is inconsistent, including the bar charts. The results of the control groups should be presented first, followed by the TMS results.

Response: Thank you for pointing this out, as it significantly improves the clarity and readability of the figures. We have revised both figures to ensure that the results of the control groups are presented first, followed by the TMS results, in all subplots.

Modification:

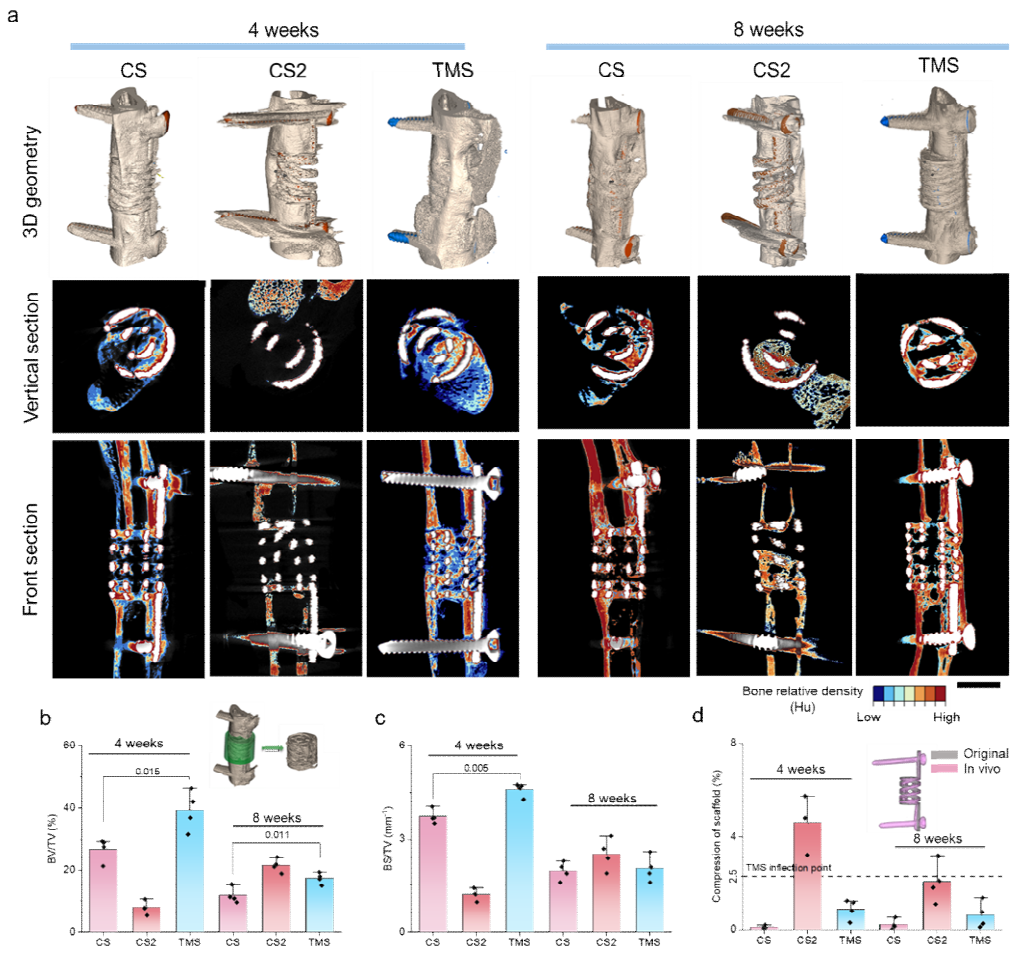

Fig. 3 TMS enhanced bone regeneration with proper tissue strain.

3. Fig. 4i contains two meaningless letters, "e".

Response: We sincerely appreciate your insightful review. We removed the two unintended letters ("e") in Fig. 4i.

Modification:

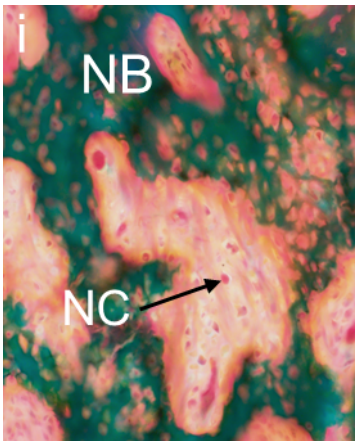

Fig. 4i Magnification of new bone growth frontiers.

4. The Western Blot data in Fig 5e should not be separated to ensure scientific accuracy; it can be replaced with Fig. S14e.

Response: We are grateful for your careful review. We agree that the Western Blot data in Fig. 5e should not be separated to ensure scientific accuracy. To address this, we have reworked the Fig.5e. The main text and supplementary materials have been updated accordingly.

Modification:

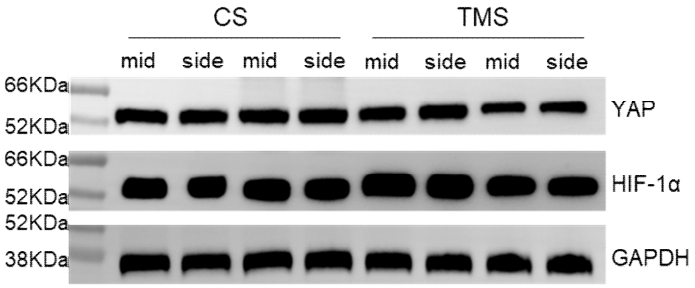

Fig. 5e Selected protein levels measured with Western blot at the middle (mid) and side of the implants (n=4).

5. An incorrect reference to Fig. S4a in Supplementary Note 4. It should be Fig.S5.

Response: We thank you for your attention to detail. The text has been modified acorrdingly.

Modification: The fatigue ratcheting and fatigue damage strain were calculated from the displacement data (Fig. S6a) according to reference [1].

Reviewer #2 (Remarks to the Author):

The study investigates the application of meta-structured scaffolds and a two-stage deformation process to enhance osteogenesis and angiogenesis. The authors conducted static and dynamic mechanical tests, along with in vivo experiments, to evaluate bone regeneration. While the study addresses an important research area, the manuscript contains several critical issues that need to be addressed to improve its scientific rigor and overall quality.

Response: Thank you for your thoughtful and constructive comments. We sincerely appreciate your recognition of the importance of our research and valuable comments. We carefully address the issues point-by-point below with the support of additional investigations and revise the manuscript accordingly.

1. The introduction of the study lacks a coherent flow and does not effectively highlight the key points of the topic. For instance, the first paragraph attempts to emphasize the importance of scaffolds, followed by statistical details from published studies, and then shifts to metamaterials without clear connections. The authors need to reorganize the introduction section to clearly outline the problem and the rationale for the study. Additionally, Fig. 1 inadequately depicts the workflow, with poorly aligned components and inconsistent sizes, and requires revision for clarity.

Response:

Thank you for your constructive feedback. We agree that the introduction requires better organization and coherence. We revised the introduction to ensure a logical flow, starting with the clinical challenges addressed by scaffolds, followed by a concise discussion of existing approaches and their mechanial limitations, leading to the rationale for introducing metamaterials in bone tissue engineering.

Regarding Fig. 1, we appreciate your observation and rework the figure to improve its alignment, component consistency. As also suggested by *Reviewer 3 comment 23*, we have incorporated the schematic diagram of the osteogenesis mechanism into Fig. 1 to more clearly depict the workflow.

Modification:

INTRODUCTION

The pursuit of low-modulus, high-strength structures [12], as well as materials [13], is essential and represents a crucial direction in current bone implant research. To overcome the mechanical limitations of existing materials, mechanical metamaterials leverage the rational design of their microstructures to achieve unique and programmable mechanical properties, such as corrugated [14], chiral [15], and auxetic materials [16]. The limited studies on metamaterial bone implants primarily focused on

auxetic materials [17, 18]. For instance, auxetic metamaterials were employed in spinal fusion for monitoring bone healing progress [19]. Additionally, the auxetic properties can enhance the pull-out resistance of bone screws [20]. Nevertheless, no significant benefits in promoting bone regeneration have been demonstrated since the existing researches on metamaterial scaffolds did not fully consider bone biomechanics. Here, we introduce a two-stage metamaterial scaffold (TMS) for critical bone defects (Fig. 1a). The scaffolds are additively manufactured with electron beam powder bed fusion (EBPBF) (Fig. 1b and Fig. S1). Such an innovative design aims to decouple the modulus and strength of the scaffold so that low modulus and high strength are achieved according to bone repairing needs. Specifically, under primary stress conditions (10N, 1/3 of the experimental animal's weight), the TMS operates in the ductile stage, showcasing a low modulus of 13 MPa and enabling sufficient strain (>1 %). Under extreme conditions (60N, 2 times the experimental animal's weight), TMS reaches the stiff stage and demonstrates adequate strength without a significant increase in strain (Fig. 1c). After in vivo implantation (Fig. 1d), The TMS exhibits a robust capacity to promote bone regeneration compared to two classic scaffolds with moduli of 500 MPa (CS) and 13 MPa (CS2), respectively. Therefore, this study demonstrates the two-stage scaffold's capability to maintain appropriate tissue strain while providing sufficient strength to address challenging critical bone defects, offering the potential to usher in a new paradigm for bone scaffold design.

[figure redacted]

Fig. 1 Workflow of the proposed metamaterial scaffold. a Structural design of a two-stage metamaterial scaffold (TMS) for critical bone defects. **b** Electron-beam 3D printing technique fabricates the proposed metallic TMS and classic scaffold (CS) design. **c** Mechanical tests demonstrate the two-stage modulus of TMS. **d** Afterwards, scaffolds are in vivo implanted in rabbits' critical ulnar defects, and TMS illustrates promotion of angiogenesis and osteogenesis.

2. The mechanical design of the TMS and CS scaffolds is unclear. Specifically, the TMS design's connection points and the rationale behind the inclusion of additional spring structures are insufficiently justified. Within the TMS structure, the two springs are connected only at a single point in the middle. If lg=0, the springs should theoretically connect along their entire length, not just at one point. Furthermore, the authors stated that dp=0 was used to create a control group, yet they previously described the addition of pillars to connect the springs. If the pillars can be removed, it raises the question of why the straight lines were designed in the first place.

Response:

Thank you for pointing out the ambiguity in the mechanical design of the TMS and CS scaffolds. We agree that the rationale for the connection points and additional spring structures requires further elaboration. As shown in Fig. 1a, the TMS is

composed of three parts: the two endfaces, the outer 4 springs and the inner 4 springs, as well as the connecting pillars between the springs. As you rightly pointed out, the key lies in the arrangement of the springs and the connections formed by the pillars.

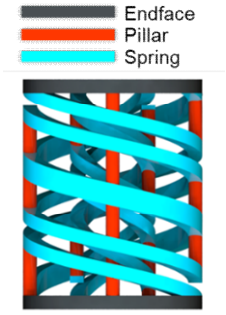

Fig. 1a Structural design of a two-stage metamaterial scaffold (TMS)

To clarify the concerns about the gap of l_g, as illustrated in Fig. R1, all springs are constructed from squares through a rotary scan process. Taking the outer ring as an example, the four springs (No.1, 2, 3, and 4) are divided into two groups: one group is marked with blue squares (No.1 and No.2), while the other group is marked with yellow squares (No.3 and No.4). When pillars are added to connect each group, the small gap (lg) of the TMS structure is formed.

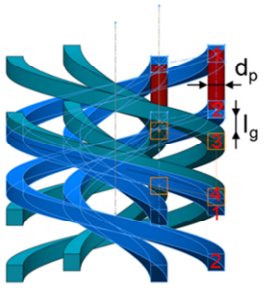

Fig. R1 Establishment of TMS springs

Therefore, yes, if lg=0, the No.2 and No.3 springs connect along their entire length, effectively forming the CS structure. However, the distance between No.1 and No.2 remains unchanged, and thus the pillars remain unaltered.

Regarding the concerns about the pillars, their role is to bear greater loads. As shown in Fig. 2g and in the supplementary video, it is clear that under small loads, the TMS structure is primarily deformed by the springs. With increased loading, the two springs gradually contact, transferring the force to the pillars. Therefore, when dp=0, the TMS structure loses its second stiff stage, retaining only the softer first-stage deformation, which becomes another control group, CS2.

We acknowledge that the previous statement in the manuscript, "The design features a variable gap between the two springs," can easily cause misunderstandings and have revised it accordingly. We also added the details of the TMS design in Supplementary Note 1 and uploaded the 3D files of TMS, CS, and CS2 to GitHub for

reference and printing.

Modification:

Mechanical design and behaviors

The design features a variable gap between the springs, denoted as l_g (Fig. 2a and Fig. S2).

Data availability

All data supporting the findings of this study are available within the article and its supplementary files. Any additional requests for information can be directed to, and will be fulfilled by, the corresponding authors. The 3D files of TMS, CS and CS2 are publicly available in the GitHub repository at https://github.com/yuqinpku/A-Metamaterial-Scaffold. Source data are provided with this paper.

Supplementary Note 1: Design and compression test

As illustrated in Fig. S1b, all springs are constructed from squares through a rotary scan process. Taking the outer ring as an example, the four springs (No.1, 2, 3, and 4) are divided into two groups: one group is marked with blue squares (No.1 and No.2), while the other group is marked with yellow squares (No.3 and No.4). When pillars are added to connect each group, the small gap (lg) of the TMS structure is formed.

3. In the sentence, "The CS displayed a stress-strain curve in compression that closely resembled that of typical bone implants (Fig. 2b)", the authors claim that CS scaffolds resemble typical bone implants, citing a reference (below) to support this assertion. The cited reference does not provide relevant stress-strain data, and the authors should instead compare their findings with the stress-strain properties of natural bone for a scientifically valid comparison.

- Reference: Z. Jia, X. Xu, D. Zhu, Y. Zheng, Design, printing, and engineering of regenerative biomaterials for personalized bone healthcare. Progress in Materials Science. 134, 101072, (2023)

Response: We sincerely thank you for pointing out this inconsistency. We acknowledge that describing the curve similarities was an imprecise expression and that specific mechanical properties should be used for comparison instead. The mechanical properties of natural bone are widely distributed, with elastic modulus ranging from 0.2-2 GPa in cancellous bone and 3-30 GPa in cortical bone. The strength varies from 5-200 MPa in different regions [2]. CS in this work (modulus ~500 MPa, strength ~30 MPa) lies within the range of mechanical properties of bone. So we also think it is also necessary to compare with current load-bearing bone defect implants, thus emphasizing the innovative properties of the TMS. As shown in Fig. R2, the lower limit of the modulus for titanium alloy implants with different pore structures is approximately 500 MPa, which is comparable to that of CS.

In the revised manuscript, we have removed the inappropriate citation and replaced it with a new reference containing stress-strain properties of bone and bone implants, as shown below.

[figure redacted]

Fig. R2. The relationship between pore and mechanical properties of Ti bone implant [r4]

Therefore, we have revised the Introduction section to introduce the mechanical properties of bone and clarified the comparison of CS with existing bones and current implants in the Mechanical design and behavior section.

[r4] C. Song, L. Liu, Z. Deng, H. Lei, F. Yuan, Y. Yang, Y. Li, Y. Jiakuo, Research progress on the design and performance of porous titanium alloy bone implants, Journal of Materials Research and Technology 23 (2023) 2626-2641.

Modification:

INTRODUCTION

However, commonly used implant metals, including titanium and its alloys, exhibit elastic moduli (approximately 110 GPa) that are significantly higher than that of natural bone (0.2-2 GPa for trabecular bone; 3-30 GPa for compact bone) [2], As a result, during loading, the majority of the stress is borne by the metal, leading to strain shielding and impaired reconstruction of the bone tissue as described by Wolff's law [3].

Mechanical design and behaviors

The CS has a modulus of only 503 MPa, which is within the range of natural bone and near the minimum modulus of Ti scaffolds for force-bearing bone implants [21].

References

[21]C. Song, L. Liu, Z. Deng, H. Lei, F. Yuan, Y. Yang, Y. Li, Y. Jiakuo, Research progress on the design and performance of porous titanium alloy bone implants, Journal of Materials Research and Technology 23, 2626-2641, (2023).

4. Based on Figs. 2b and 2c, these figures should correspond to TMS and CS, respectively. However, in Fig. 2d, the colors and behaviors differ from those in the earlier figures, creating inconsistency. More critically, a small toe region is observable in Fig. 2b but is absent in Fig. 2d, raising concerns about the accuracy of the results. Interestingly, this small toe region reappears in Fig. 2e, further complicating the interpretation. If CS exhibits a toe region with two-stage deformation, what then differentiates CS from TMS? Additionally, why was the CS2 configuration not shown separately for clarity and comparison?

Response:

Thank you for this comment. Regarding the issues with the toe region, the mentioned toe region is very common in the compression performance testing of 3D-

printed metal scaffolds. As shown in Fig. R2a and R2b, this phenomenon occurs because the contact surface between the printed metal sample and the compression head is very rough. During compression testing, these small protrusions are preferentially compressed and yield before the scaffold itself bears the load. However, when the loading surface is polished, the compressive force directly acts on the scaffold itself, and this phenomenon disappears (Fig. R3c) [r5].

[figure redacted]

Fig. R3 Compression curves of different titanium porous supports. **a** and **b** as-built sample [r6, r7], **c** samples after machining [r5]

Therefore, this CS toe region due to the roughness is irrecoverable, as shown in Fig. 2e in this paper. In contrast, the low modulus stage in TMS is caused by the elastic deformation of the spring, which is continuously recoverable to meet the demand of cyclic loading for bone implant.

As for the concerns of inconsistency of toe region in Fig. 2b and 2d, this is due to the visual difference caused by the difference in the axis scales. To clarify this, we submitted the source data of all figures in the revised paper. Specifically, the source data of CS (strain 0-5%)is shown below.

The modulus of CS2 is 13.3±0.1 MPa, closely matching the first-stage modulus (E1) of TMS, which is 13.4±2.2 MPa. However, without the second stage, CS2 fails to enhance osteogenesis compared to TMS. In this work, CS2 was designed to demonstrate that low modulus alone cannot facilitate osteogenesis and is not intended to represent traditional implants. Therefore, for CS2, the most important modulus was shown in the main text to illustrating the advantages of TMS's two-stage design. And other characteristics were placed it in the supplementary materials to avoid potential distraction of readers.

Table R1 Compression stress-strain dataset of CS with three replicates

CS-1		CS-2		CS-3	
Strain	Stress	Strain	Stress	Strain	Stress
-0.006	-0.006	-0.01	#####	-0.007	0.0861
-0.003	-	-0.007	-	-0.005	0.0857
0.015	0.0050	0.009	0.0153	0.011	0.0929
0.031	0.0216	0.025	0.0400	0.028	0.1052
0.043	0.0254	0.04	0.0486	0.042	0.1119
0.056	0.0346	0.053	0.0605	0.053	0.1244
0.07	0.0500	0.064	0.0668	0.067	0.1295
0.079	0.0578	0.077	0.0757	0.079	0.1450
0.093	0.0724	0.09	0.0871	0.092	0.1567
0.106	0.0898	0.102	0.1017	0.102	0.1736
0.117	0.1048	0.113	0.1129	0.116	0.1910
0.13	0.1150	0.127	0.1303	0.13	0.1997
0.142	0.1275	0.14	0.1478	0.14	0.2153
0.156	0.1352	0.15	0.1588	0.154	0.2292
0.166	0.1434	0.165	0.1767	0.165	0.2372
0.18	0.1552	0.176	0.1935	0.178	0.2468
0.193	0.1710	0.189	0.2138	0.189	0.2624
0.203	0.1790	0.2	0.2270	0.203	0.2779
0.217	0.1955	0.213	0.2478	0.217	0.2870
0.229	0.213	0.227	0.2679	0.226	0.3108
0.242	0.2272	0.236	0.2749	0.24	0.3236
0.252	0.2411	0.252	0.2968	0.252	0.3439
0.266	0.2615	0.263	0.3122	0.265	0.3602
0.28	0.2813	0.275	0.3250	0.275	0.3803
0.289	0.2951	0.286	0.3413	0.289	0.4005
0.304	0.3135	0.3	0.3611	0.303	0.4118
0.315	0.3332	0.314	0.3820	0.312	0.4380
0.328	0.3585	0.323	0.3891	0.327	0.4558
0.339	0.3778	0.338	0.4135	0.339	0.4771
0.353	0.4114	0.349	0.4280	0.351	0.4998
0.366	0.4382	0.361	0.4405	0.362	0.5167
0.375	0.4571	0.373	0.4617	0.375	0.5425
0.39	0.4828	0.386	0.4769	0.39	0.5549
0.402	0.5041	0.4	0.5016	0.399	0.5792
0.414	0.5198	0.409	0.5080	0.414	0.5962
0.426	0.5346	0.424	0.5312	0.425	0.6152
0.439	0.5449	0.436	0.5439	0.437	0.6330
0.453	0.5505	0.447	0.5573	0.449	0.6517
0.462	0.5551	0.46	0.5742	0.462	0.6719
0.477	0.5815	0.472	0.5999	0.476	0.6864
0.489	0.5979	0.486	0.6184	0.485	0.7144
0.499	0.6180	0.496	0.6367	0.5	0.7367
0.513	0.6453	0.511	0.6663	0.512	0.7581
0.526	0.6762	0.523	0.6782	0.523	0.7935
0.539	0.7121	0.534	0.6946	0.536	0.8251
0.549	0.7315	0.546	0.7134	0.548	0.8574
0.563	0.7758	0.559	0.7278	0.561	0.8925
0.576	0.8088	0.572	0.7487	0.572	0.9441
0.586	0.8397	0.583	0.7580	0.586	0.9763
0.6	0.8782	0.597	0.7805	0.598	1.0012
0.612	0.9053	0.609	0.7935	0.609	1.0454
0.625	0.9401	0.62	0.8042	0.622	1.0787
0.635	0.9619	0.633	0.8234	0.635	1.1209
0.649	1.0065	0.646	0.8368	0.648	1.1581
0.663	1.0325	0.659	0.8515	0.659	1.1966
0.672	1.0534	0.669	0.8581	0.673	1.2348
0.687	1.0891	0.683	0.8765	0.686	1.2665
0.699	1.1106	0.696	0.8882	0.695	1.3212
0.71	1.1377	0.706	0.8964	0.709	1.3649
0.723	1.1618	0.72	0.9226	0.722	1.4003
0.735	1.2017	0.732	0.9543	0.734	1.4505
0.749	1.2490	0.745	0.9922	0.745	1.4888
0.758	1.2693	0.756	1.0253	0.758	1.5430
0.773	1.3185	0.77	1.0640	0.772	1.5695
0.786	1.3581	0.783	1.0943	0.781	1.6225
0.797	1.3962	0.793	1.1174	0.796	1.6755
0.81	1.4395	0.807	1.1533	0.808	1.7159
0.822	1.4926	0.819	1.1871	0.819	1.7766
0.835	1.5540	0.831	1.2253	0.832	1.8316
0.845	1.5843	0.843	1.2534	0.845	1.8953
0.86	1.6511	0.856	1.2841	0.858	1.9363
0.873	1.7021	0.869	1.3149	0.868	2.0070
0.883	1.7422	0.879	1.3258	0.882	2.0822
0.897	1.8057	0.893	1.3592	0.895	2.1239
0.908	1.8546	0.906	1.3803	0.906	2.2045
0.921	1.9064	0.917	1.3979	0.919	2.2641
0.931	1.9467	0.93	1.4226	0.931	2.3172
0.946	2.0181	0.942	1.4442	0.944	2.3734
0.96	2.0699	0.956	1.4757	0.954	2.4543
0.969	2.1035	0.965	1.4858	0.969	2.5289
0.983	2.1759	0.98	1.5212	0.982	2.5723
0.995	2.2198	0.993	1.5411	0.992	2.6619
1.007	2.2684	1.003	1.5601	1.006	2.7239
1.019	2.3095	1.017	1.5900	1.018	2.7795
1.032	2.3649	1.029	1.6159	1.03	2.8493
1.046	2.4116	1.042	1.6473	1.041	2.9248
1.055	2.4387	1.052	1.6656	1.055	2.9998
1.07	2.503	1.066	1.6941	1.069	3.0515
1.082	2.5470	1.079	1.7176	1.078	3.1327
1.093	2.5953	1.089	1.7398	1.092	3.199
1.105	2.6434	1.104	1.7757	1.104	3.2620
1.119	2.7108	1.115	1.7976	1.116	3.3498
1.132	2.7809	1.127	1.8291	1.128	3.4322
1.142	2.8094	1.139	1.8506	1.141	3.5131
1.157	2.8907	1.152	1.8898	1.155	3.5795
1.168	2.9364	1.167	1.9349	1.164	3.6816
1.179	2.9891	1.176	1.9646	1.179	3.7590
1.192	3.0480	1.191	2.0206	1.191	3.8177
1.205	3.1095	1.203	2.0501	1.202	3.9279
1.218	3.1769	1.213	2.0930	1.215	3.9991
1.228	3.2057	1.226	2.1340	1.227	4.0762
1.243	3.2980	1.239	2.2037	1.241	4.1512
1.255	3.3605	1.253	2.2622	1.251	4.2347
1.265	3.4219	1.262	2.2964	1.265	4.3159
1.279	3.4988	1.276	2.3638	1.278	4.3712
1.292	3.5797	1.289	2.4081	1.288	4.4758
1.304	3.6462	1.299	2.4526	1.302	4.5520
1.315	3.6957	1.313	2.4983	1.314	4.6093
1.329	3.7981	1.326	2.5610	1.327	4.6850
1.342	3.8667	1.338	2.6227	1.338	4.7606
1.352	3.9252	1.349	2.6572	1.352	4.8373
1.365	4.0046	1.363	2.7263	1.364	4.886
1.378	4.0733	1.376	2.7826	1.374	4.9853
1.39	4.1582	1.385	2.8179	1.388	5.0582
1.402	4.2104	1.4	2.8793	1.402	5.1241
1.415	4.3003	1.412	2.9281	1.413	5.2089
1.428	4.3631	1.424	2.9892	1.425	5.2964
1.437	4.4024	1.436	3.0284	1.438	5.3947
1.452	4.4936	1.449	3.1038	1.451	5.4550
1.466	4.5759	1.462	3.1672	1.461	5.5765
1.476	4.6516	1.472	3.2046	1.476	5.6656
1.489	4.7164	1.487	3.2805	1.488	5.7325
1.501	4.8080	1.5	3.3425	1.499	5.8483
1.515	4.8981	1.511	3.3993	1.512	5.9212
1.525	4.9517	1.523	3.4544	1.525	6.0195
1.539	5.0638	1.536	3.5252	1.537	6.0891
1.552	5.1462	1.549	3.5884	1.546	6.1867
1.562	5.2273	1.558	3.6210	1.561	6.2902
1.575	5.3170	1.573	3.6987	1.575	6.3455
1.588	5.4237	1.587	3.7667	1.585	6.4803
1.601	5.5254	1.596	3.8157	1.599	6.5563
1.611	5.5838	1.61	3.8958	1.61	6.6530
1.625	5.7063	1.622	3.9647	1.623	6.7337
1.638	5.7887	1.635	4.0384	1.633	6.8633
1.648	5.8853	1.645	4.0844	1.648	6.9752
1.662	5.9864	1.66	4.1731	1.662	7.0258

1.674	6.0909	1.673	4.2369	1.672	7.1713	2.787	19.453	2.785	13.357	2.783	19.705	3.899	28.704	3.895	28.079	3.896	31.721
1.688	6.2067	1.683	4.2914	1.685	7.2585	2.797	19.565	2.794	13.442	2.797	19.869	3.908	28.667	3.909	28.187	3.908	31.813
1.697	6.2659	1.697	4.3638	1.697	7.3598	2.812	19.737	2.809	13.633	2.809	19.962	3.924	28.788	3.921	28.324	3.922	31.800
1.711	6.3989	1.709	4.4323	1.71	7.4632	2.823	19.875	2.822	13.775	2.82	20.189	3.936	28.802	3.934	28.451	3.931	31.912
1.725	6.5060	1.721	4.5033	1.72	7.5845	2.836	20.040	2.832	13.919	2.833	20.354	3.946	28.808	3.944	28.497	3.945	31.990
1.735	6.5942	1.732	4.5497	1.734	7.7170	2.848	20.128	2.846	14.057	2.846	20.491	3.96	28.853	3.958	28.679	3.959	31.957
1.749	6.7094	1.746	4.6400	1.748	7.7689	2.861	20.314	2.857	14.210	2.859	20.668	3.972	28.907	3.972	28.787	3.969	32.081
1.761	6.8270	1.76	4.7207	1.757	7.9209	2.874	20.463	2.871	14.416	2.869	20.834	3.985	28.960	3.981	28.844	3.983	32.085
1.773	6.9512	1.769	4.7571	1.772	8.0176	2.883	20.543	2.881	14.526	2.883	21.009	3.995	28.926	3.996	28.972	3.994	32.134
1.784	7.0329	1.784	4.8545	1.784	8.1028	2.898	20.744	2.896	14.761	2.896	21.107	4.009	29.011	4.007	29.091	4.007	32.131
1.798	7.2025	1.795	4.9096	1.796	8.2128	2.91	20.901	2.908	14.912	2.906	21.338	4.022	29.026	4.02	29.213	4.017	32.222
1.812	7.3335	1.807	4.9798	1.807	8.3204	2.922	21.050	2.918	15.046	2.921	21.507	4.033	29.025	4.031	29.230	4.032	32.286
1.821	7.4237	1.819	5.0324	1.82	8.4425	2.934	21.153	2.932	15.222	2.933	21.607	4.047	29.075	4.044	29.402	4.045	32.218
1.835	7.5686	1.832	5.1241	1.835	8.4902	2.947	21.326	2.945	15.394	2.944	21.810	4.059	29.085	4.058	29.499	4.055	32.334
1.847	7.6923	1.846	5.2069	1.844	8.6385	2.96	21.474	2.957	15.579	2.956	21.972	4.071	29.125	4.068	29.545	4.069	32.333
1.86	7.8407	1.855	5.2531	1.859	8.7085	2.969	21.554	2.969	15.685	2.969	22.166	4.082	29.073	4.082	29.684	4.081	32.360
1.871	7.9258	1.87	5.3541	1.871	8.7888	2.984	21.755	2.982	15.901	2.983	22.278	4.096	29.168	4.094	29.754	4.094	32.375
1.884	8.0799	1.882	5.4214	1.882	8.8981	2.997	21.887	2.995	16.069	2.992	22.504	4.11	29.186	4.106	29.871	4.104	32.432
1.898	8.1888	1.893	5.498	1.893	9.0161	3.008	22.019	3.004	16.194	3.007	22.670	4.119	29.132	4.117	29.876	4.118	32.465
1.907	8.2390	1.906	5.5600	1.907	9.1364	3.02	22.133	3.019	16.417	3.019	22.781	4.134	29.207	4.13	30.034	4.131	32.403
1.923	8.4096	1.919	5.6524	1.921	9.1948	3.033	22.325	3.032	16.591	3.031	23.004	4.145	29.183	4.145	30.141	4.141	32.506
1.934	8.5171	1.932	5.7353	1.93	9.3538	3.046	22.469	3.043	16.767	3.043	23.161	4.157	29.215	4.154	30.147	4.157	32.498
1.946	8.6679	1.942	5.7853	1.945	9.4545	3.056	22.534	3.055	16.895	3.056	23.332	4.169	29.179	4.169	30.283	4.168	32.474
1.958	8.7775	1.957	5.9017	1.957	9.5445	3.071	22.740	3.068	17.103	3.069	23.440	4.182	29.247	4.18	30.321	4.18	32.512
1.97	8.9538	1.969	5.9738	1.968	9.6922	3.083	22.852	3.082	17.300	3.078	23.686	4.196	29.261	4.192	30.416	4.191	32.514
1.984	9.1205	1.98	6.0543	1.981	9.8124	3.094	22.972	3.091	17.401	3.093	23.892	4.205	29.181	4.204	30.430	4.204	32.564
1.994	9.2139	1.992	6.1399	1.993	9.9536	3.108	23.103	3.106	17.649	3.107	23.970	4.22	29.252	4.218	30.563	4.218	32.500
2.009	9.4110	2.005	6.2314	2.007	10.025	3.12	23.249	3.118	17.814	3.117	24.213	4.232	29.233	4.232	30.659	4.228	32.574
2.021	9.5480	2.019	6.3371	2.016	10.180	3.133	23.400	3.129	17.975	3.13	24.332	4.243	29.226	4.24	30.617	4.243	32.563
2.032	9.6974	2.028	6.3955	2.031	10.317	3.143	23.463	3.142	18.149	3.142	24.502	4.256	29.224	4.255	30.753	4.254	32.493
2.044	9.8305	2.043	6.5349	2.044	10.401	3.156	23.640	3.154	18.353	3.155	24.627	4.268	29.245	4.267	30.794	4.265	32.567
2.057	10.027	2.056	6.6169	2.054	10.576	3.17	23.778	3.168	18.563	3.165	24.827	4.282	29.249	4.279	30.864	4.278	32.563
2.071	10.213	2.065	6.6933	2.068	10.710	3.18	23.878	3.177	18.659	3.18	25.028	4.292	29.179	4.291	30.881	4.291	32.562
2.081	10.313	2.079	6.7966	2.08	10.843	3.195	24.026	3.192	18.909	3.193	25.086	4.306	29.248	4.304	30.982	4.305	32.513
2.095	10.526	2.092	6.9136	2.093	10.970	3.206	24.143	3.205	19.100	3.202	25.336	4.319	29.216	4.317	31.046	4.314	32.546
2.107	10.669	2.105	7.0287	2.103	11.145	3.218	24.275	3.215	19.256	3.217	25.458	4.329	29.173	4.327	31.024	4.329	32.550
2.118	10.821	2.115	7.0843	2.118	11.303	3.229	24.328	3.23	19.450	3.229	25.590	4.343	29.173	4.342	31.173	4.341	32.459
2.131	10.984	2.129	7.2232	2.13	11.396	3.243	24.510	3.241	19.633	3.241	25.746	4.355	29.174	4.354	31.172	4.352	32.545
2.144	11.170	2.142	7.3088	2.14	11.576	3.258	24.651	3.253	19.813	3.252	25.919	4.368	29.190	4.365	31.209	4.365	32.509
2.156	11.346	2.152	7.3937	2.154	11.712	3.267	24.678	3.264	19.941	3.266	26.101	4.379	29.104	4.377	31.226	4.378	32.475
2.167	11.455	2.166	7.5056	2.166	11.861	3.281	24.832	3.279	20.193	3.279	26.165	4.392	29.151	4.39	31.311	4.39	32.448
2.181	11.682	2.179	7.6074	2.18	11.987	3.293	24.931	3.292	20.383	3.289	26.409	4.405	29.119	4.404	31.395	4.401	32.455
2.194	11.840	2.19	7.7252	2.19	12.142	3.305	25.064	3.301	20.497	3.304	26.520	4.415	29.036	4.414	31.347	4.415	32.469
2.204	11.975	2.202	7.8021	2.204	12.305	3.316	25.115	3.316	20.723	3.316	26.651	4.429	29.069	4.428	31.477	4.428	32.371
2.218	12.165	2.216	7.9369	2.217	12.391	3.33	25.278	3.328	20.883	3.327	26.804	4.442	29.059	4.441	31.482	4.438	32.439
2.23	12.320	2.229	8.0356	2.227	12.593	3.344	25.412	3.339	21.066	3.339	26.963	4.454	29.018	4.451	31.475	4.452	32.398
2.243	12.518	2.238	8.1156	2.241	12.746	3.353	25.434	3.351	21.194	3.352	27.148	4.466	28.957	4.465	31.529	4.464	32.328
2.254	12.636	2.253	8.2454	2.253	12.878	3.367	25.588	3.365	21.429	3.366	27.221	4.478	28.968	4.477	31.583	4.477	32.348
2.267	12.845	2.265	8.3424	2.266	13.053	3.38	25.683	3.379	21.629	3.375	27.431	4.492	28.939	4.49	31.643	4.488	32.310
2.281	13.020	2.277	8.4666	2.277	13.185	3.391	25.795	3.388	21.702	3.39	27.549	4.501	28.854	4.501	31.594	4.501	32.312
2.29	13.132	2.289	8.5559	2.289	13.380	3.403	25.842	3.403	21.947	3.402	27.633	4.516	28.885	4.514	31.675	4.514	32.221
2.305	13.345	2.302	8.6872	2.304	13.474	3.416	25.987	3.415	22.085	3.413	27.793	4.529	28.849	4.528	31.700	4.523	32.259
2.318	13.509	2.315	8.7992	2.313	13.690	3.43	26.106	3.425	22.263	3.426	27.958	4.539	28.772	4.537	31.676	4.538	32.242
2.328	13.663	2.325	8.867	2.328	13.840	3.439	26.129	3.439	22.423	3.439	28.090	4.553	28.739	4.552	31.750	4.551	32.164
2.341	13.822	2.339	8.9940	2.34	13.945	3.454	26.293	3.451	22.615	3.453	28.163	4.565	28.723	4.564	31.769	4.562	32.187
2.353	13.991	2.352	9.106	2.351	14.127	3.466	26.357	3.465	22.811	3.462	28.353	4.578	28.700	4.575	31.780	4.575	32.131
2.367	14.176	2.363	9.2125	2.364	14.271	3.477	26.448	3.474	22.906	3.477	28.468	4.588	28.591	4.587	31.760	4.587	32.096
2.376	14.284	2.376	9.3003	2.376	14.439	3.489	26.497	3.489	23.160	3.489	28.549	4.602	28.623	4.601	31.838	4.601	32.038
2.392	14.519	2.388	9.4277	2.39	14.559	3.502	26.631	3.502	23.310	3.499	28.713	4.615	28.559	4.614	31.856	4.61	32.069
2.405	14.680	2.401	9.5372	2.4	14.741	3.516	26.773	3.511	23.445	3.513	28.833	4.626	28.489	4.624	31.802	4.625	32.048
2.415	14.812	2.411	9.6134	2.414	14.905	3.526	26.770	3.525	23.615	3.525	28.950	4.64	28.464	4.638	31.879	4.638	31.924
2.428	14.978	2.426	9.7615	2.426	15.002	3.541	26.939	3.538	23.813	3.538	29.018	4.652	28.424	4.65	31.865	4.648	31.961
2.44	15.145	2.439	9.8668	2.437	15.211	3.552	26.981	3.551	24.025	3.548	29.197	4.664	28.374	4.662	31.891	4.661	31.905
2.453	15.347	2.449	9.9712	2.451	15.333	3.563	27.051	3.561	24.108	3.563	29.321	4.674	28.265	4.675	31.877	4.673	31.865
2.463	15.436	2.462	10.077	2.463	15.498	3.576	27.120	3.575	24.353	3.575	29.360	4.689	28.296	4.687	31.911	4.687	31.815
2.478	15.674	2.474	10.205	2.476	15.627	3.589	27.243	3.588	24.483	3.586	29.555	4.703	28.250	4.7	31.928	4.697	31.828
2.491	15.821	2.488	10.347	2.486	15.828	3.602	27.348	3.598	24.617	3.599	29.639	4.712	28.134	4.71	31.846	4.712	31.797
2.5	15.942	2.498	10.422	2.5	16.019	3.612	27.324	3.612	24.807	3.611	29.755	4.727	28.131	4.724	31.944	4.724	31.678
2.515	16.151	2.512	10.586	2.514	16.117	3.626	27.481	3.625	24.975	3.624	29.848	4.738	28.046	4.738	31.945	4.734	31.710
2.527	16.295	2.525	10.704	2.524	16.345	3.639	27.534	3.637	25.165	3.635	29.989	4.75	28.011	4.748	31.897	4.749	31.651
2.539	16.481	2.535	10.815	2.538	16.483	3.65	27.580	3.648	25.245	3.649	30.120	4.761	27.910	4.762	31.924	4.76	31.589
2.55	16.577	2.55	10.957	2.549	16.628	3.664	27.661	3.662	25.481	3.662	30.131	4.775	27.916	4.773	31.909	4.773	31.573
2.564	16.782	2.561	11.087	2.562	16.792	3.675	27.736	3.675	25.623	3.671	30.299	4.789	27.865	4.786	31.943	4.784	31.517
2.578	16.957	2.574	11.240	2.572	16.978	3.688	27.815	3.684	25.723	3.686	30.408	4.798	27.737	4.797	31.860	4.797	31.511
2.587	17.049	2.585	11.323	2.587	17.170	3.699	27.803	3.699	25.924	3.699	30.482	4.813	27.741	4.811	31.960	4.811	31.415
2.602	17.252	2.598	11.487	2.6	17.256	3.713	27.954	3.711	26.061	3.71	30.576	4.825	27.667	4.825	31.943	4.821	31.444
2.614	17.379	2.612	11.627	2.609	17.473	3.726	27.987	3.723	26.220	3.722	30.677	4.836	27.605	4.834	31.868	4.836	31.380
2.625	17.522	2.622	11.715	2.624	17.638	3.736	27.998	3.735	26.308	3.735	30.777	4.848	27.514	4.848	31.912	4.847	31.272
2.637	17.643	2.637	11.863	2.636	17.751	3.75	28.072	3.748	26.524	3.748	30.796	4.861	27.500	4.86	31.892	4.858	31.275
2.651	17.850	2.648	11.974	2.648	17.946	3.762	28.140	3.761	26.655	3.758	30.968	4.876	27.448	4.872	31.911	4.87	31.244
2.664	18.015	2.66	12.102	2.66	18.103	3.775	28.213	3.771	26.735	3.773	31.050	4.884	27.323	4.884	31.845	4.884	31.204
2.674	18.087	2.671	12.177	2.672	18.265	3.786	28.210	3.785	26.927	3.785	31.075	4.9	27.338	4.897	31.905	4.898	31.104
2.688	18.291	2.685	12.339	2.687	18.385	3.799	28.321	3.798	27.058	3.796	31.174	4.911	27.242	4.911	31.885	4.907	31.109
2.7	18.417	2.699	12.476	2.696	18.595	3.813	28.369	3.809	27.205	3.809	31.256	4.923	27.177	4.92	31.800	4.922	31.055
2.711	18.546	2.708	12.552	2.711	18.762	3.822	28.358	3.822	27.314	3.822	31.377	4.935	27.097	4.935	31.870	4.934	30.957
2.724	18.681	2.723	12.719	2.722	18.852	3.836	28.461	3.835	27.473	3.835	31.357	4.947	27.065	4.947	31.822	4.945	30.970
2.737	18.858	2.734	12.826	2.733	19.065	3.849	28.504	3.847	27.604	3.844	31.505	4.962	27.025	4.958	31.807	4.957	30.920
2.75	19.023	2.746	12.960	2.746	19.220	3.86	28.546	3.857	27.659	3.859	31.565	4.971	26.888	4.97	31.764	4.971	30.864
2.76	19.101	2.758	13.057	2.759	19.393	3.873	28.559	3.872	27.852	3.871	31.580	4.986	26.891	4.983	31.788	4.983	30.773
2.774	19.327	2.772	13.199	2.773	19.514	3.885	28.632	3.886	27.991	3.882	31.701	4.998	26.727	4.997	31.806	4.993	30.776

[r5] Y. Chen, J.E. Frith, A. Dehghan-Manshadi, H. Attar, D. Kent, N.D.M. Soro, M.J. Bermingham, M.S. Dargusch, Mechanical properties and biocompatibility of porous titanium scaffolds for bone tissue engineering, Journal of the Mechanical Behavior of Biomedical Materials 75 (2017) 169-174.

[r6] J. Wieding, A. Jonitz, R. Bader, The Effect of Structural Design on Mechanical Properties and Cellular Response of Additive Manufactured Titanium Scaffolds, Materials, 5(8) (2012) 1336-1347.

[r7] C.-H. Tsai, C.-H. Hung, C.-N. Kuo, C.-Y. Chen, Y.-N. Peng, M.-Y. Shie, Improved Bioactivity of 3D Printed Porous Titanium Alloy Scaffold with Chitosan/Magnesium-Calcium Silicate Composite for Orthopaedic Applications, Materials,12 (2019), 203.

Modification:

Data availability

All data supporting the findings of this study are available within the article and its supplementary files. Any additional requests for information can be directed to, and will be fulfilled by, the corresponding authors. The 3D files of TMS, CS and CS2 are publicly available in the GitHub repository at https://github.com/yuqinpku/A-Metamaterial-Scaffold. Source data are provided with this paper.

5. Based on the following paragraph in the manuscript, how did the authors confirm osteogenesis? Detailed justification and evidence are required to support these claims.
- "The TMS demonstrates an effective modulus of only 13.4 MPa, producing an inflection point strain of 2.5% with a small force of 10 N. Additional compressive forces result in the stiff stage of the TMS, where the modulus reaches 318 MPa. When subjected to a total force of 60 N (twice the animal's body weight), the strain is still within 5%, thus ensuring both strength and osteogenesis".

Response: We thank you for the valuable comment. We recognize that mentioning osteogenesis in the "Mechanical design and behaviors" section appears abrupt, as osteogenesis is confirmed in subsequent sections on radiographics, histology, and proteomics. Therefore, we have removed the mention of osteogenesis here and revised it to " demonstrating both strong and elastic capacity."

Modification:

Mechanical design and behaviors

When subjected to a total force of 60 N (twice the animal's body weight), the strain is still within 5%, demonstrating both strong and elastic capacity.

6. The three-point bending test in Fig. S3 includes additional parts to control movement, which could affect scaffold properties. The rationale behind these design choices and their alignment with standard protocols should be clarified.

Response: We cordially thank you for this comment. According to ISO 7438:2020 - Metallic materials - Bend test-Standard, the length of the test specimen is at least 2.5 times greater than the diameter. But our scaffolds not match the length the standard. At the same time, the ends of scaffolds are difficult to fix due to the small diameter of the springs (<500 μm). Therefore, in this study, we decided to approach the experiment from a practical application perspective by conducting three-point bending tests on samples used in vivo with plates added for screw fixation. This loading method more closely mimics in vivo conditions, as the bending force is not directly transmitted through the scaffold ends but rather through the plate. In the Materials and Methods section, we have added a detailed description of the test samples to clarify the

experimental establishment.

Modification:

MATERIALS AND METHODS

In vivo implanted scaffolds were used for testing to closely mimics in vivo conditions. Two supports were added on the plates and the load was perpendicularly added to the axis of the scaffolds.

7. According to the paragraph, "However, the TMS has a decreasing fatigue damage strain, which indicates that the TMS has a certain work hardening effect during fatigue tests. Both compression unloading and fatigue tests demonstrated the resilience of TMS. In short, the TMS exhibits tunable, two-stage compression behavior and maintains resilience well under fatigue loading," the authors suggest that TMS has superior fatigue properties compared to CS. However, based on the strain values presented in Fig. 2, CS exhibits lower deformation after 80,000 cycles, implying that CS may demonstrate better long-term durability. This apparent contradiction raises questions about the interpretation of the fatigue test results and the potential for earlier failure of TMS under similar fatigue conditions.

Response:

We sincerely appreciate your critical feedback. However, please allow us to respectfully disagree with the comment "the authors suggest that TMS has superior fatigue properties compared to CS". As you mentioned, CS exhibits lower deformation compared with TMS. In the main text, we also claimed this deformation is cyclic ratcheting for both groups and "the cyclic ratcheting strain value of TMS was higher than that of CS."

In the fatigue testing, we think the most significant findings are as follows: First, TMS can withstand one million cyclic loads while maintaining its two-stage deformation behavior, ensuring that the designed nonlinear mechanical properties can provide sustained biomechanical support during the two-month bone reconstruction process. Second, the difference of fatigue performance between TMS and CS is noteworthy. As mentioned in the text, TMS undergoes negative fatigue damage, whereas CS exhibits a sudden increase in fatigue damage under high circles. Meanwhile, the ratcheting damage of TMS is exponentially higher than CS. Generally, fatigue damage leads to catastrophic failure of the sample, whereas ratcheting damage results in loss of support due to excessive deformation. In short, both TMS and CS demonstrated sufficient redundancy of fatigue property for in vivo application, but their fatigue pattern differs from each other. To avoid misunderstanding of readers that TMS outperforms CS, we revised the text to clarify the above information.

Modification:

Mechanical design and behaviors

Regarding the performance of compression fatigue (Fig. 2k-2n and Fig. S6), both TMS and CS demonstrated sufficient redundancy in fatigue properties for in vivo applications, but their fatigue behaviors showed distinctive features. Notably, the TMS structure successfully endured one million compression cycles with a load twice the animal's body weight, and still retained its two-stage characteristics. CS exhibited a sudden increase in fatigue damage after approximately 80,000 cycles. Whereas TMS underwent negative fatigue damage, suggesting a certain work hardening effect during fatigue tests. Meanwhile, TMS structure predominantly exhibited ratcheting damage exponentially higher than CS. In short, the TMS exhibits tunable, two-stage compression behavior and maintains good resilience under fatigue loading.

8. In the sentences, "The geometry differences among CS, CS2, and TMS are the small gap (lg) and pillar (dp) as mentioned before. Thus, except for the mechanical properties, the impact of other geometry factors on osteogenesis, such as pore size [20, 21], curvature [22, 23], and porosity [9], can be neglected," the authors dismiss the influence of key geometric factors on osteogenesis. However, the geometry differences, such as variations up to 0.25 mm, are substantial enough to significantly affect mechanical properties. It is therefore scientifically inconsistent to assume that these changes have negligible effects on osteogenesis.

Response:

Thank you for this insightful comment. Firstly, the designed porosity of CS, CS2 and TMS is 77.8%, 78.8% and 78.5 %, respectively. And the as-built porosity of CS, CS2 and TMS calculated from micro-CT is 73.3±0.3 % 74.1±0.5 % and 73.1±0.2 % , respectively. Therefore, we believe that the porosity of the three scaffolds can be considered identical and does not affect osteogenesis. In fact, the differences between these three structures lie in the slight overlap of two springs (CS and TMS) or the struts between springs (CS and CS2), which do not significantly impact porosity.

As for pore size, since the TMS structure is not composed of a typical periodic unit, measuring pore size as defined by the diameter of the largest sphere that fits inside the pore and contains the voxel [r8] is not applicable to this structure. To control pore size, we added the same endface as shown in Fig. R4, thus ensure that the pore size along the bone growth direction was identical among the three structures.

The geometry difference between TMS and two CSs is designed to change its mechanical properties. For example, the gap l_g = 0.25 mm, thus the TMS can have its two-stage deformation bevaviors.

In fact, as we mentioned in the manuscript, there are many structural parameters influencing osteogenesis. Even though many studies currently declare only one of these parameters [r9], the other parameters are acturally interrelated, making it challenging to control variables. For example, based on the Gibson-Ashby model, the elastic modulus of porous structures:

$$E=E_0 D^n$$

Where E_0 is elastic modulus of the fully dense material (base material without porosity).

D is the relative density (equals one minus porosity, ranging from 0 to 1). And *n* is empirical constant (depends on the material and structure, typically between 2 and 4 for cellular solids).

Thus as also shown in Fig.R2, to achieve a 10-times change in modulus within traditional cellular structures, the density would need to increase 2.2 times (n=3). At this point, it becomes difficult to attribute the difference in osteogenesis to either mechanical properties or pore size. Other methods like changing the unit structure to achieve a wide mechanical range is even less feasible, as it would completely change the pore shape, size, and other characteristics.

Therefore, this study uses the simple modification of TMS into CS as a control group instead of selecting an existing structure from the literature. We believe this approach provides significantly better control over other geometry parameters. Consequently, we consider it reasonable to disregard the effects of other structural factors in this context. In the revised paper, we declared the porosity of three scaffolds.

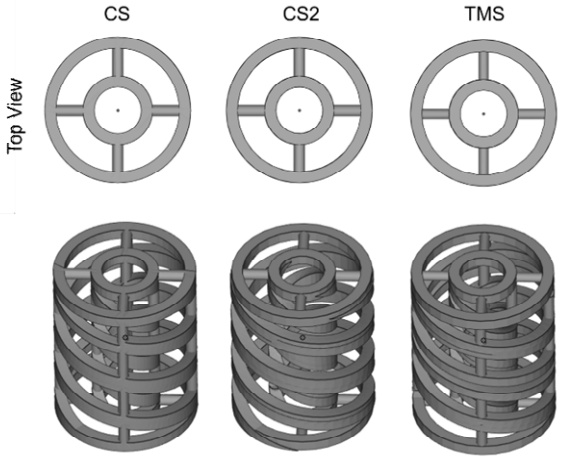

Fig. R4 Structural comparsion of scaffolds

[r8]. N. Taniguchi, S. Fujibayashi, M. Takemoto, K. Sasaki, B. Otsuki, T. Nakamura, T. Matsushita, T. Kokubo, S. Matsuda, Effect of pore size on bone ingrowth into porous titanium implants fabricated by additive manufacturing: An in vivo experiment. Materials Science and Engineering: C. 59, 690-701, (2016)

[r9] S.S. Lee, X. Du, I. Kim, S.J. Ferguson, Scaffolds for bone-tissue engineering, Matter 5(9) (2022) 2722-2759

Modification:

Supplementary Note 1: Design and compression test

The designed porosity of CS, CS2 and TMS is 77.8%, 78.8% and 78.5 %, respectively. And the as-built porosity of CS, CS2 and TMS calculated from micro-CT is 73.3±0.3 % 74.1±0.5 % and 73.1±0.2 %, respectively.

9. The differences between CS and TMS in Fig. S7 are not clearly discernible at the current resolution. To effectively highlight these distinctions, higher-magnification imaging should be employed.

Response: Thank you for pointing this out. We revised this figure with enlarged pictures. In this paper, X-ray imaging was caputured with live rabbits, which primarily focuses on assessing bone morphology to evaluate deformities and major complications such as fractures or ulnar-radial fusion. For a more detailed evaluation of bone formation, micro-CT imaging was used to provide clear and more comprehensive insights.

Modification:

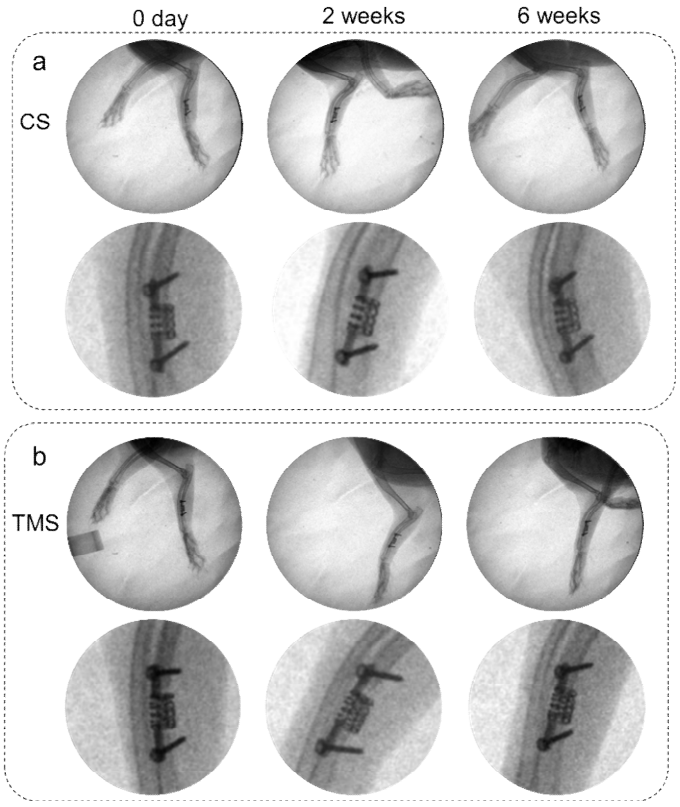

Fig S8 X-ray images of implanted CS and TMS at 0, 2 and 6 weeks. a CS. b TMS.

10. In TMS structures, a small lg creates small pores in the scaffolds, which could influence the bone healing process. In contrast, the larger pore size in CS structures may lack the same potential to accelerate bone regeneration, as shown in Figs. 3 and 4. Additionally, these differences, along with variations in porosity, could impact the modulus of the newly formed bone due to the stress shielding effect. To comprehensively evaluate the TMS and CS structures, it is essential to consider all relevant variables, including pore size, porosity, and their potential biological and mechanical impacts.

Response: We thank you for your insightful comment. We think concerns of porosity, pore size and mechainical properties can be refered to the response of *Review 2, Comment 8*. Besides, we also agree that the side pores of TMS can potentially affecting osteogenesis. However, as answered in *Review 2, Comment 11.3*, the small gap (l_g) introduced in the TMS structure actually lacked bone formation due to excessive

mechanical strain. Therefore, these small pores did not provide TMS with an advantage over CS in terms of osteogenesis.

11 In the discussion section, finite element modeling (FEM) was utilized to simulate the strain behavior of bone tissue during osteogenesis. However, in the "Mechanical Tests and Simulations" section, the focus is primarily on the mechanical properties of the main scaffolds. According to Fig. 6, the simulation incorporates both the scaffolds and bone tissue, using the mechanical properties of the callus to represent bone tissue during early osteogenesis (as described in "Tissue Strain Analysis").
This raises several important questions:
11.1 Why were the specific mechanical properties of the callus chosen for the simulation?

Response: We thank you for this comment. The choice of callus mechanical properties was based on the specific biological context of early osteogenesis. During the bone defect healing process, callus forms a temporary tissue structure and provides mechanical stability and supporting in facilitating new bone formation. Meanwhile, callus tissue is the first non-inflammatory tissue to experience mechanical forces after a bone defect, and it plays a critical role in determining subsequent osteocyte mineralization, as well as the regeneration of woven and compact bone [r10, r11]. Thus, the strain behavior of callus tissue is essential and decisive when studying the process of bone regeneration [r12]. And also in this study, simulations of tissue strain at different stages of osteogenesis were also conducted as shown in Fig. 6d and Fig. S16.

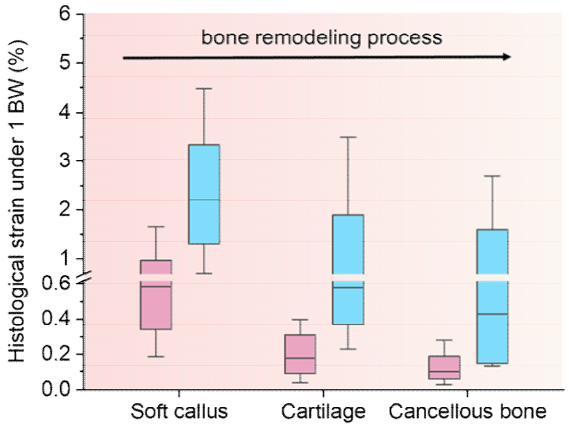

Fig. 6d Bone tissue strain analysis and compressive properties of bone implants.

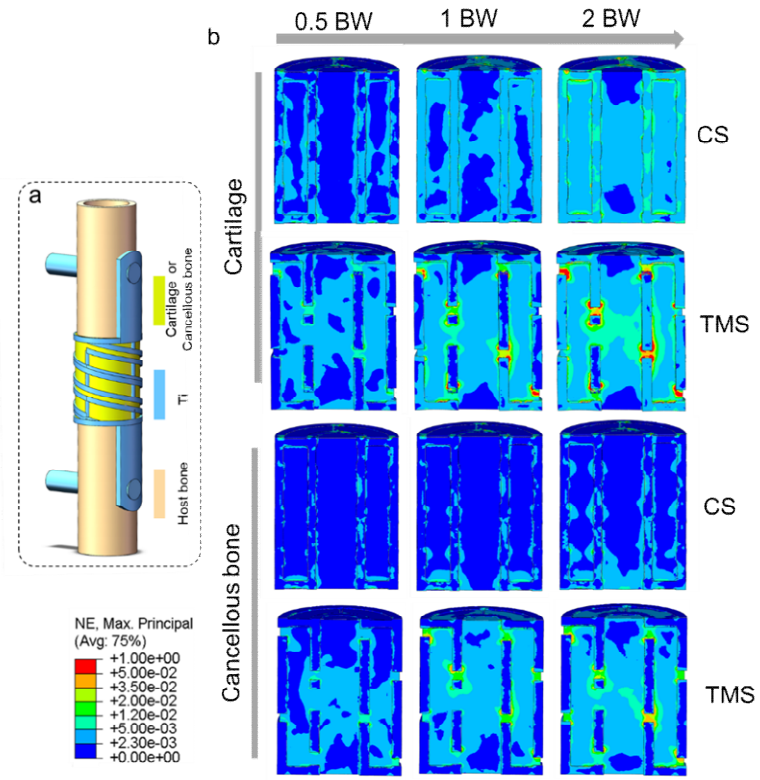

Fig. S16 FEM of the defect after cartilage or cancellous bone regeneration. a Illustration of implanted TMS with bone tissue. **b, c** Maximum principal strains of CS and TMS within the cartilage or cancellous bone and scaffolds under different the body weight

[r10] D.R. Epari, J. Lienau, H. Schell, F. Witt, G.N. Duda, Pressure, oxygen tension and temperature in the periosteal callus during bone healing—An in vivo study in sheep, Bone 43(4) (2008) 734-739.
[r11] G.N. Duda, S. Geissler, S. Checa, S. Tsitsilonis, A. Petersen, K. Schmidt-Bleek, The decisive early phase of bone regeneration, Nature Reviews Rheumatology 19(2) (2023) 78-95.
[r12] A.-M. Pobloth, S. Checa, H. Razi, A. Petersen, J.C. Weaver, K. Schmidt-Bleek, M. Windolf, A.Á. Tatai, C.P. Roth, K.-D. Schaser, G.N. Duda, P. Schwabe, Mechanobiologically optimized 3D titanium-mesh scaffolds enhance bone regeneration in critical segmental defects in sheep. Science Translational Medicine. 10(423), eaam8828, (2018)

11.2 Did the authors account for the interaction between the scaffolds and host tissue in their modeling approach?

Response: Thank you for the kind remind. Yes, the interaction between the scaffolds and host tissue was considered in the modeling approach. Specifically, the model incorporated boundary conditions that ties the surface of scaffold and the surrounding host tissue together. We add this information in the revised paper.

Modification:

Tissue strain analysis

The surfaces of the scaffold and bone tissue were modeled with tie-constraints to simulate their physical interaction in Abaqus/Explicit.

11.3. Most critically, the study did not validate the FEM results with experimental data, which is essential to confirm the accuracy and reliability of the simulations.
Addressing these points would greatly enhance the scientific rigor and reliability of the findings.

Response:

Thank you for highlighting this important point. We have included the simulation comparision to experiment of compression tests in the reviesed paper. Detailed description can be found later in *Review 2, Comment 13*. But measuring tissue strain in vivo is highly challenging, as even after sacrificing the rabbits, only the strain on the surface of the sample can be measured, making it difficult to analyze the strain distribution throughout the entire scaffold space. Therefore, single simulation of tissue strain is common in researches as described before. In this paper the simulation can effectively demonstrated the significant differences in strain distribution between TMS and CS. Additionally, we think the histological results provide strong evidence supporting the reliability of our simulations. For instance, as shown below in Fig.R5, regions within the TMS scaffold center with simulated strains between 0.0023 and 0.05 exhibited significantly higher levels of bone formation. Conversely, regions at the small gap of l_g exceeding 5% strain showed reduced bone formation.

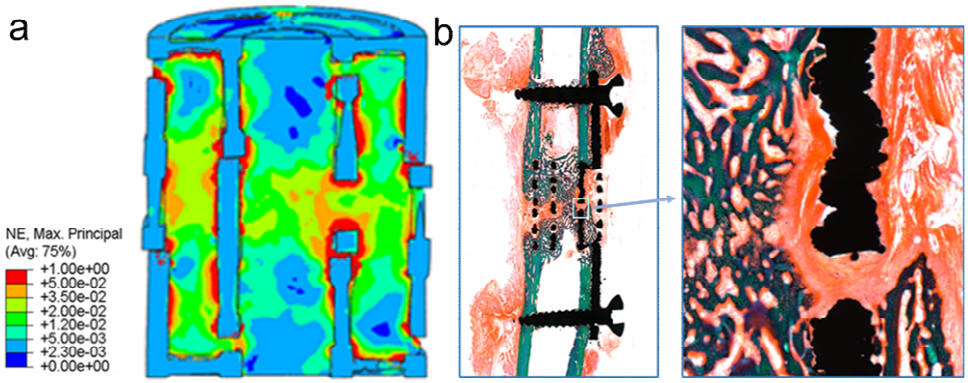

Fig.R5 **a** Maximum principal strains within the soft callus tissue of TMS. **b** Histomorphological evaluations of TMS at 4 weeks.

12. One major concern in the present study is the quality and resolution of the 3D printing process, which was not adequately addressed in the results or discussion. Poor printing quality can significantly impact the structural integrity and performance of the scaffolds, potentially compromising the reliability of the results. To evaluate the printing accuracy, SEM images of the fabricated scaffolds should be compared with the designed models. Additionally, Fig. S1 reveals indications of low printing quality, which further emphasizes the need for a detailed assessment of the manufacturing process and its implications on the study's findings.

Response:

Thank you for this insightful comment. We agree that the quality and resolution of the 3D printing process play a crucial role in determining the structural integrity of the scaffolds. To address this concern, we have conduct additional experiments and include cross-sectional SEM images of the fabricated TMS alongside their designed models in Supplementary Fig. S1c as below.

In the context of 3D-printed titanium alloy scaffolds, printing quality contains multiple aspects, with two key factors being forming density and forming accuracy [r13, r14]. In this work, the scaffolds prepared using EBPBF exhibit high formation density, with negligible internal porosity. Using an image-based method [r15], we calculated the relative density to exceed 99.9%. This demonstrates the reliability of the scaffold's forming density.

We understand that this comment may be more concerned with printing accuracy. By comparing the cross-section of the printed scaffold with the original design, the scaffold retained its designed geometry with an area overlap ratio of 92%, and the additional area accounted for 23%, as shown in Fig.S1c. This surface inaccuracy, caused by powder adhesion, is a common phenomenon in 3D-printed titanium alloys. While techniques such as hydrofluoric acid treatment can reduce roughness, they may pose safety concerns. In fact, the unpolished scaffolds with our fabrication methods have already been used in clinical applications, demonstrating good therapeutic outcomes [r16].

In this study, we utilized a commercial EBPBF machine shown in Fig.S1d to print titanium alloy scaffolds. We think the most critical factor is the forming density, which ensures sufficient strength. Furthermore, the mechanical experiments showed that the two-stage mechanical performance of the TMS was unaffected by forming accuracy. Thus the TMS does not require specialized printing processes or equipment, which we believe is an enhancement of the accessibility and clinically translational potential.

[r13] L.-C. Zhang, Y. Liu, S. Li, Y. Hao, Additive Manufacturing of Titanium Alloys by Electron Beam Melting: A Review, Advanced Engineering Materials 20(5) (2018) 1700842.

[r14] S. Wang, J. Ning, L. Zhu, Z. Yang, W. Yan, Y. Dun, P. Xue, P. Xu, S. Bose, A. Bandyopadhyay, Role of porosity defects in metal 3D printing: Formation mechanisms, impacts on properties and mitigation strategies, Materials Today 59 (2022) 133-160.

[r15] P. Wen, M. Voshage, L. Jauer, Y. Chen, Y. Qin, R. Poprawe, J.H. Schleifenbaum, Laser additive manufacturing of Zn metal parts for biodegradable applications: Processing, formation quality and mechanical properties, Materials & Design 155 (2018) 36-45.

[r16] T. Zhang, Q. Wei, H. Zhou, Z. Jing, X. Liu, Y. Zheng, H. Cai, F. Wei, L. Jiang, M. Yu, Y. Cheng, D. Fan, W. Zhou, X. Lin, H. Leng, J. Li, X. Li, C. Wang, Y. Tian, Z. Liu, Three-dimensional-printed individualized porous implants: A new “implant-bone” interface fusion concept for large bone defect treatment, Bioactive Materials 6(11) (2021) 3659-3670

Modification:

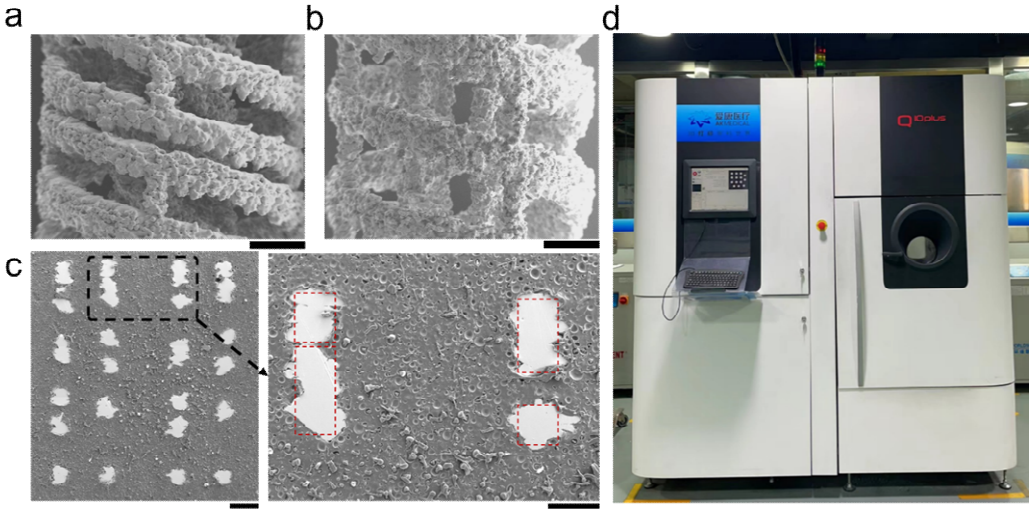

Fig. S1 a and b, SEM pictures of as-built TMS and CS scaffolds, respectively. Scale bars = 1 mm **c** Cross-sectional view of as- built TMS compared with designed structure (dashed box). scale bar = 1 mm and 500 μm, respectively. **d** EBPBF machine

13. In the "Mechanical Tests and Simulations" section, the authors did not adhere to a standard protocol for calculating the mechanical properties of the scaffolds or for evaluating the non-porous materials used in the FEM simulations. This lack of standardization raises concerns about the reliability, consistency, and comparability of the mechanical property data and its subsequent use in FEM modeling.

Response:

Thank you for this valuable comment. We agree that following a standardized protocol for calculating the mechanical properties is crucial for ensuring the reliability and consistency of the results. To address this concern, we have now included a detailed description of the calculation methods and the evaluation protocols used in the "Mechanical Tests and Simulations" section. Specifically, we have referenced standardized approaches for determining mechanical properties.

Additionally, we have included a comparison of the simulated results and experimental data as shown below. The simulated modui for the two stages are within the range of the experimental data. As shown below and in Fig. 2d, the simulated modulus for the first stage is 14.3 MPa, while the experimental data is 13.4 ± 2.2 MPa. For the second stage, the simulated modulus is 338 MPa, compared to the experimental value of 318 ± 30 MPa. The difference between and experiment is inflection point strain: the simulation is lager than experiments. This discrepancy is due to the fact that, as shown in Fig. S1, the additively manufactured samples have a rougher and more uneven surface than the designed surface, causing the actual l_g to be smaller than the design value. Regarding the material properties used in the simulation, titanium alloy is a common engineering material. We used publicly available parameters for titanium alloy, specifically a Young's modulus of 116 GPa with a Poisson's ratio of 0.30 [r17], as inputs for the simulation. On one hand, the use of these readily available data is considered

reliable and has been widely applied in studies on 3D printed titanium alloy bone implants [r18-r20]. On the other hand, the good match between our simulation and experimental results also helps validate the effectiveness of the chosen parameters. In the revised manuscript, we have added a detailed comparison between the simulation and experimental results to clarify the above points.

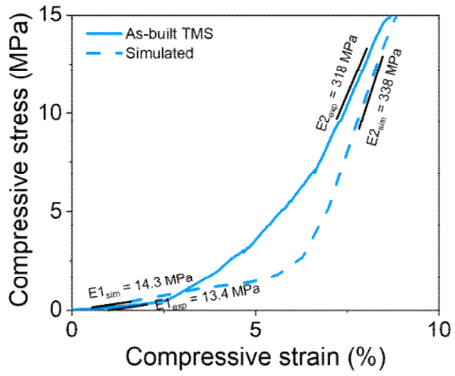

Fig. S17 The simulated strain-stress curves of TMS compared with experiments

[r17] S. Anupam, An Overview of Metallic Biomaterials for Bone Support and Replacement, in: N.L. Anthony (Ed.), Biomedical Engineering, IntechOpen, Rijeka, 2011, p. Ch. 7.
[r18] A.-M. Pobloth, S. Checa, H. Razi, A. Petersen, J.C. Weaver, K. Schmidt-Bleek, M. Windolf, A.Á. Tatai, C.P. Roth, K.-D. Schaser, G.N. Duda, P. Schwabe, Mechanobiologically optimized 3D titanium-mesh scaffolds enhance bone regeneration in critical segmental defects in sheep. Science Translational Medicine. 10(423), eaam8828, (2018)
[r19] B. Liu, Q. Tan, Z. Wang, G. Hou, C. Wang, Y. Tian, Applying 3D-Printed Porous Ti6Al4V Prostheses to Repair Osteomyelitis-Induced Partial Bone Defects of Lower Limbs: Finite Element Analysis and Clinical Outcomes, 2025. https://doi.org/10.1111/os.14268.
[r20] S. Brogini, A. Crovace, A. Piccininni, G. Serratore, G. Marchiori, M. Maglio, P. Guglielmi, A. Cusanno, L. De Napoli, R. Conte, M. Fini, G. Ambrogio, G. Palumbo, G. Giavaresi, In vivo validation of highly customized cranial Ti-6AL-4V ELI prostheses fabricated through incremental forming and superplastic forming: an ovine model study, Scientific Reports 14(1) (2024) 7959.

Modification:

Mechanical tests and simulations

The quasi-static compression tests were carried out using a universal material testing machine (Instron 5969, USA) with a 100 kN load cell under room temperature. The loading rate was 0.5 mm/min, corresponding to an initial strain rate of 0.001/s according to ASTM E9-19. During compression tests, the strain of scaffolds was

recorded using a digital image correlation (DIC) system (XTDIC-2D, China). To ensure the reliability and reproducibility of the results, each sample was tested in triplicate.

Afterwards, the finite element modeling (FEM) of compression was conducted on a 32-core and 64-thread CPU (Intel Xeon Gold 6226R Processor) using Abaqus/Explicit software (Dassault Corp, French). The FEM was based on two rigid load cell and deformable-implant-structure model to simulated the compression experiments [12]. The Ti material was set as homogeneous with a poisson ratio of 0.3. Young's modulus and yield strength of Ti were set as 116 GPa and 600 MPa, respectively. The simulated and experimental stress-strain curves are plotted in Fig. S17. In post-processing, the von-Mise stress under different strain was used to analyze the mechanical behaviors.

Supplementary Note 11: Compression simulation accuracy

As shown in Fig. S16 and Fig. 2d, the simulated modulus for the first stage is 14.3 MPa, while the experimental value is 13.4 ± 2.2 MPa. For the second stage, the simulated modulus is 338 MPa, compared to the experimental value of 318 ± 30 MPa. The primary discrepancy between the simulation and experimental results lies in the inflection point strain, which is larger in the simulation. This difference arises because, as illustrated in Fig. S1, the additively manufactured samples have rougher and more uneven surfaces compared to the designed surfaces, resulting in an actual l_g that is smaller than the design value.

Reviewer #3 (Remarks to the Author):

I co-reviewed this manuscript with one of the reviewers who provided the listed reports. This is part of the Nature Communications initiative to facilitate training in peer review and to provide appropriate recognition for Early Career Researchers who co-review manuscripts.

Response: Thank you for your contribution and input.

Reviewer #4 (Remarks to the Author):

The paper is well researched and the concept is very novel and timely. Although several papers have published on metamaterials, 3D printed bone implants and both combined, the idea of a metamaterial with different properties over different mechanical regimes is very well developed in this paper. The figures are all well-presented and very well organized and detailed. I suggest a number of minor corrections before the paper can be accepted for publication. There are some sections in the introduction that need a bit of rewriting, in particular including more detail on referenced work to provide a clearer picture of the current state-of-the-art in the field. Some parts of the materials and methods section need more detail, both to understand the presented data better and to allow researchers to replicate the body of work. Also in the results there are a few sections that need more clarification and corrections.
These points are highlighted in more detail below:

Response: We are most grateful to you for the strong support of our work and also for the very pertinent comments, which help us profoundly to improve the quality of our manuscript. We have carefully addressed the issues point-by-point and we revised the manuscript accordingly. The detailed responses are given below.

1.Introduction
Line 40-41 "modulus of metal" is too vague considering how many metals there are. Be more specific in defining the metals used for bone implants and how it relates to bone tissue engineering.

Response: We thank you for the valuable comment. We include details on the specific titanium metals used for bone implants and further describe how their modulus affects bone regeneration.

Modification: However, commonly used implant metals, including titanium and its alloys, exhibit elastic moduli (approximately 110 GPa) that are significantly higher than that of natural bone (0.2-2 GPa for trabecular bone; 3-30 GPa for compact bone) [2], As a result, during loading, the majority of the stress is borne by the metal, leading to strain shielding and impaired reconstruction of the bone tissue as described by Wolff's law [3].

2.47-48 "optimised osteogenesis" in terms of what, osteoblast proliferation, callus formation. The finding is not necessarily because of the callus formation, that is simply an observation.
Response: We appreciate your insightful comment. We have revised the text to clarify

that the reported optimized osteogenesis is related to endochondral and intramembranous ossification.

Modification: Pobloth et al. designed scaffolds with varying moduli for treating critical bone defects. They determined the minimum-modulus scaffold of 840 MPa has optimized endochondral and intramembranous ossification, due to a maximum strain of surrounding callus tissue up to 0.6% [6].

3. 49 reconstruction may be the wrong word given it indicates human intervention rather than on its own healing

Response: Thank you for this very insigthful comment. We have replaced "reconstruction" with "regeneration". We agree that "reconstruction" implies intervention, such as surgery or the use of scaffolds, while "regeneration" more accurately reflects the natural healing process of bone. Therefore, we have also revised the relevant sections throughout the manuscript to ensure consistency and clarity.

Modification: . While theoretical simulations suggest that 0.23-5% callus tissue strains promote bone regeneration [6-8], tissue strains greater than 1% has been regarded unattainable in vivo

4. In general the references in the main body of text accurately describe whats happening in the text but may need more explanation of exactly why they were used.

Response: Thank you for your comment. We have revised the manuscript and added detailed information where reference was used, and illustrate their relevance to the points discussed in the text.

5. Some of the English reads poorly. For example in lines 58-59, the use of "specially architectured" and "properties beyond" are not especially descriptive and require revision.

Response: Thank you for pointing this out. We carefully re-check and improve the language of the entire manuscript. The sentences you mentioned was rewritten more specificly describe metamaterials.

Modification: To overcome the mechanical limitations of existing materials, mechanical metamaterials leverage the rational design of their microstructures to achieve unique and programmable mechanical properties, such as corrugated [14], chiral [15], and auxetic materials [16].

6. 60-61 should explain exactly why specific geometries are non-conducive to osteogenesis, in order to better set up why the proposed design is more effective according to the study.

Response: Thank you for pointing this out. We include additional explain why other metameterials are non-conducive to osteogenesis.

Modification: The limited studies on metamaterial bone implants primarily focus on auxetic materials. For instance, auxetic metamaterials have been employed in spinal fusion for monitoring bone healing progress. Additionally, the auxetic properties can enhance the pull-out resistance of bone screws. Since the design of existing mechanical metamaterials is not based on bone biomechanics, no significant benefits in promoting bone regeneration have been demonstrated.

7. "The TMS exhibits a robust capacity to promote bone reconstruction compared to two classic scaffolds (CS with modulus of 500 MPa, CS2 with modulus of 13 MPa)", SHOULD READ "The TMS exhibits a robust capacity to promote bone reconstruction compared to two classic scaffolds with moduli of 500 MPa (CS) and 13 MPa (CS2) respectively."

Response: Thank you for your suggestion. We modified the text accordingly.

Modification: The TMS exhibits a robust capacity to promote bone regeneration compared to two classic scaffolds with moduli of 500 MPa (CS) and 13 MPa (CS2), respectively.

8. Although this body of work can be considered novel it is worth mentioning some of the fabrication, characterisation and testing of metamaterial based bone tissue engineering scaffolds, as data does exist out there outside of the referenced papers in the study.

Response: Thank you for your recognition. In the revised paper, we have supplemented data of the fabrication including additive manufacturing parameters: Also we conducted additional formation quality characterization of TMS cross section as shown below and also in Fig. S1.

Modification:

Materials and additive manufacturing

We fabricated the Ti6Al4V (Ti) scaffolds using an electron beam powder bed fusion

(EBPBF) system (Q10plus, Arcam AB, Sweden). Typically, cylindrical CS and TMS scaffolds were converted into a standard triangulation language (STL) file and transferred to the EBPBF machine. The Ti powder (particle diameter: 45–100 μm) [12] was melted layer by layer according to the STL data and solidified by cooling afterward. The beam current was set as 28mA. Scanning speed was 1200 mm/s. Linear energy was 1.4 J/mm. Slicing layer height is 0.05mm. All prepared scaffolds were ultrasonically cleaned for 15 minutes in acetone, ethyl alcohol, and deionized water.

Supplymentary Note 1

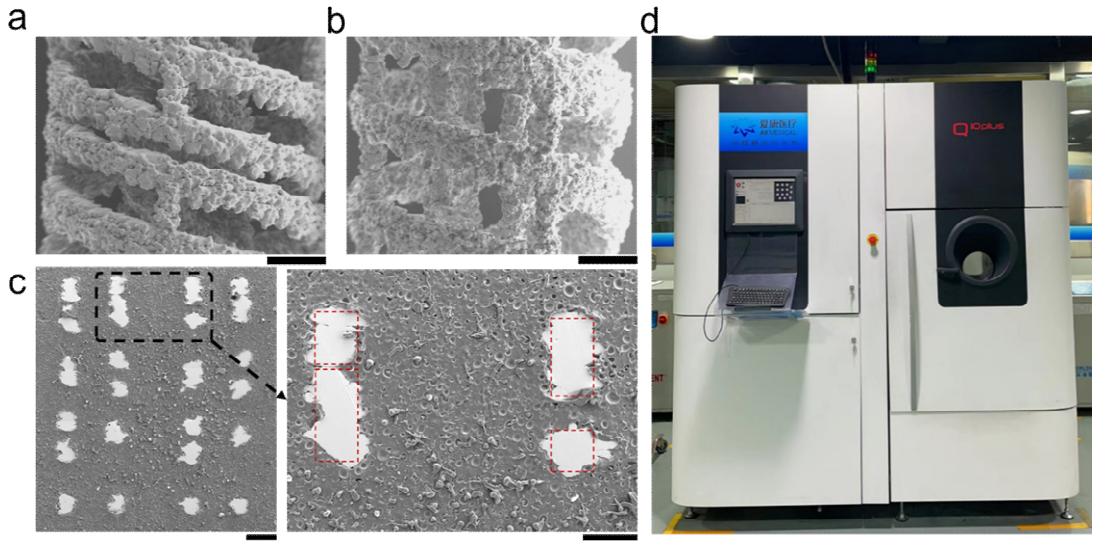

Fig. S1 a and b, SEM pictures of as-built TMS and CS scaffolds, respectively. Scale bars = 1 mm **c** Cross-sectional view of as- built TMS compared with designed structure (dashed box). scale bar = 1 mm and 500 μm, respectively. **d** EBPBF machine

9.Materials and Methods Section

As a general rule in all the materials and methods the amount of technical and biological replicates needs to be provided (n=? N=?). There are some references to repeats in the main text but this should also be provided in the methods section for clarity.

Response: Thank you for the valuable suggestion. We add the numbers of replicates where missed in this section. And generally, we modified the whole section to present a more specific description of the entire experiment.

Modification:

Mechanical tests and simulations

To ensure the reliability and reproducibility of the results, each sample was tested in triplicate.

Three-point bending tests were performed at room temperature using the same

machine (Instron 5969) with three replicates.

Fatigue tests were performed on an all-electric dynamic test instrument (Instron E3000, USA) with a frequency of 10 Hz with three replicates.

Western blot assay

In the Western blot test, two rabbits were selected from each group of TMS and CS, and bone tissue was collected from both the middle and the side of the scaffold for each rabbit.

10. Materials and Additive Manufacturing- more detail needed in terms of printing parameters. This includes the beam current, scan speed, linear energy, cooling speed and the slicing layer height.

Response: Thank you for the valuable suggestion. We add the printing parameters in the reviesed paper. The beam current is 28mA. Scanning speed is 1200 mm/s. Linear energy is 1.4 J/mm. Slicing layer height is 0.05mm. The cooling speed is not a controllable parameter during our printing. According to literature[r21,r22], the cooling rate of EBPBF is generally around 10^3-10^5K/s. The printing parameters are added in the revised paper. We also added the EBPBF machine and powder information.

[r21] K. Mizuta, Y. Hijikata, T. Fujii, K. Gokan, K. Kakehi, Characterization of Ti-48Al-2Cr-2Nb built by selective laser melting, Scripta Materialia 203 (2021) 114107.
[r22] S.S. Al-Bermani, M.L. Blackmore, W. Zhang, I. Todd, The Origin of Microstructural Diversity, Texture, and Mechanical Properties in Electron Beam Melted Ti-6Al-4V, Metallurgical and Materials Transactions A 41(13) (2010) 3422-3434.

Modification:

Materials and additive manufacturing

The beam current was set as 28mA. Scanning speed was 1200 mm/s. Linear energy was 1.4 J/mm. Slicing layer height is 0.05mm.

11. Mechanical tests and simulations- there needs to be a mention of the type, model and force rating of the load cell used in this experiment. Consider in the future performing the mechanical testing at the intended operation temperature instead of ambient.

Response: Thank you for the valuable comment. We add the detailed information such as load cell, load rate and simulation model details in the revised paper. We change “ambient” to “room temperature” in accordance with bending tests and apologize for the neglect of recording temperature. For reference, the mechanical tests of TMS and

CS were all carried out from May to June, 2023, Beijing, China. And CS2 were added at May, 2024, the same location. The room temperature at that time is generally between 20-28 degrees. As you suggest, we will record it in the future.

Modification:

The quasi-static compression tests were carried out using a universal material testing machine (Instron 5969, USA) with a 100 kN load cell under room temperature according to ASTM E9-19. The loading rate was 0.5 mm/min, corresponding to an initial strain rate of 0.001/s. During compression tests, the strain of scaffolds was recorded using a digital image correlation (DIC) system (XTDIC-2D, China). To ensure the reliability and reproducibility of the results, each sample was tested in triplicate.

Afterwards, the finite element modeling (FEM) of compression was conducted on a 32-core and 64-thread CPU (Intel Xeon Gold 6226R Processor) using ABAQUS/Explicit software. The FEM was based on two rigid load cell and deformable-implant-structure model to simulated the compression experiments []. The Ti material was set as homogeneous with a poisson ratio of 0.3. Young's modulus and yield strength of Ti were set as 116 GPa and 600 MPa, respectively. In post-processing, the von-Mise stress under different strain was used to analyze the mechanical behaviors.

12. Animal model establishment- Lines 376 and 377 mention the generation of a defect but how was this defect produced. Line 381 should read "the rest of"

Response:

We appreciate your careful review. The ulnar defect is established with follow steps. First, anesthetize the rabbit using pentobarbital sodium (30 mg kg−1, i.p.). Afterwards, each rabbit's left anterior limb was fixed, shaved, and depilated. An incision around 30 mm was made parallel to the ulna. The muscles were then bluntly separated along the intermuscular space, exposing the middle part of the diaphysis. Using a pendulum saw, a bone defect approximately 10 mm in length at the middle part of the diaphysis was created. The scaffold was implanted inside afterwards and fixed with two Ti6Al4V bone screws of 1.6 mm in diameter and 12 mm in length.

The manuscript and your mentioned grammar mistake in Line 381 was resived accordingly.

Modification:

Lines 376: The surgical procedures were performed with the rabbits under general anaesthesia using pentobarbital sodium (30 mg kg−1, i.p.). Each rabbit's left anterior limb was fixed, shaved, and depilated. An incision around 30 mm was made parallel to the ulna. The muscles were then bluntly separated along the intermuscular space,

exposing the middle part of the diaphysis. Using a pendulum saw, a bone defect approximately 10 mm in length at the middle part of the diaphysis was created as shown in Fig. S6b. The scaffold was implanted inside afterwards and fixed with two Ti6Al4V bone screws of 1.6 mm in diameter and 12 mm in length (Libeier, China) as shown in Fig. S6c.

Line 381: 8 weeks after surgery, the rest of 12 rabbits were euthanized for radiographic analysis and histological analysis.

13. Radiographic analysis- software should be cited in-text. There should be a description exactly what value Hounsfield units denotes both bone, soft tissue and the implant.

Response:

Thank you for this comment. We added the softerware information for CT reconstruction.

Hounsfield units is a relative measurement of linear attenuation coefficient. We found a silight diffence of HU (about 100 HU) to divided of different tissues may due to the sample distance to the radiation source or bone mass. For example in Fig. R6 below, the lower boundary HU of cancellous bone in TMS-1 is 580 HU, and 492 HU for TMS-2. To more accurately divide the tissues, the protocol contains 3 steps as shown below. Step A, find the lowest and highest values of HU in the bone tissue regiron; Step B, divide the HU intervals of the bone tissue and assign them to the heat map; Step C, get the CT section with bone density differentiation. This protocol is also added in the revised paper.

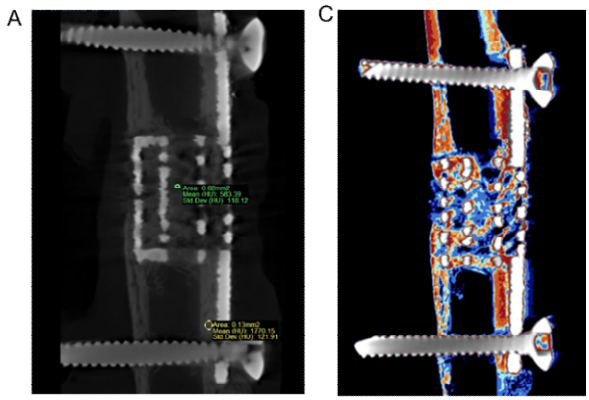

Fig. R6 Protocol of divison bone density with Hounsfield units

Modification:

The micro-CT DICOM images were then reconstructed using Mimics software (Mimics Medical 21.0, France). The bone was distinguished from soft tissue and titanium implants by partitioning different Hounsfield units (HUs). Firstly, the lowest and highest values of HUs were determined in the bone tissue region. Then the HU intervals of the bone tissue were divided and assign them to the heat map.

14. Nanoindentation- other parameters that need to be described are the displacement, displacement rate and the distance between each indentation for single samples.

Response: Thank you for this comment. The nanoindentation is a force loading pattern rather than displacement according to ISO 14577 standard. We think the reason is displacement loading pattern encountered in localized hard areas can lead to mechanical exceedance and indenter damage. In this work, a maximum load of 50 mN was applied longitudinally at a constant loading rate of 1.6 mN/s, following a holding time of 10 s. And tissue with different hardness has different depth and depth rate as shown in Fig. S13 below. As for the distance between each indentation, at least five indentations were made in the host bone, new bone, and osteoid areas of each specimen. In the selected tissue area, the indentations were arranged in a grid pattern with a spacing of 300 μm.

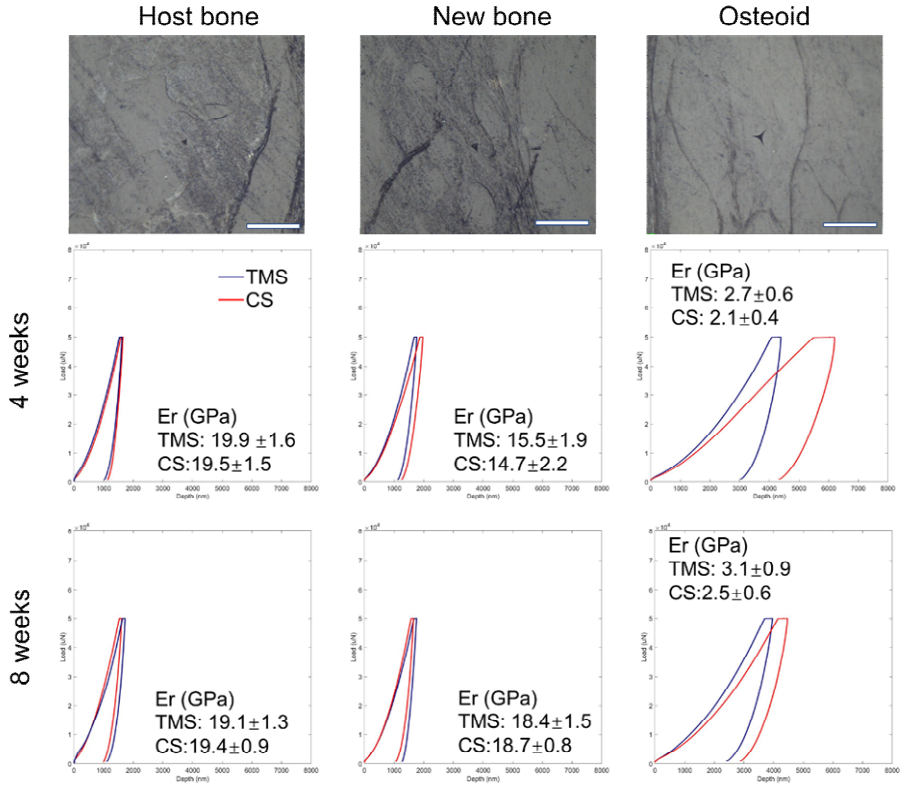

Fig. S13 Reduced modulus of bone tissues via nanoindentation tests.

Modification: At least five indentations were made in the host bone, new bone, and osteoid areas of each specimen. In the selected tissue area, the indentations were

arranged in a grid pattern with a spacing of 300 μm.

15.2nd harmonic generation imaging- the number of measurements taken per image and the number of images used is required.

Response: Thank you for your comment. We have added the required details in the revised manuscript.

Modification: Two osteoid-rich regions were selected for each sample for SHG image capture. The SHG signal was generated with an 860 nm-wavelength laser. The SHG signal was detected in the range of 410 to 450 nm (that is, half-excitation wavelength). Images were recorded using a 40× objective with a scanning resolution of 512 x 512. The acquisition time of each image was set as 10 s.

6.Western blot and proteomics analysis. Much more detail in terms of parameters, timings etc for both of these methods. Good examples of methods sections demonstrating the level of detail (https://doi.org/10.1186/s13036-021-00273-6, https://doi.org/10.1016/j.bone.2011.09.039 and https://doi.org/10.1038/s41598-020-75527-2). Please note I do not ask these references to be added to the manuscript they are just examples of detailed methods sections.

Response: Thank you for your valuable and informative comment. We have added more detailed information regarding the parameters, timings, and other specifics for both Western blot and proteomics analysis, following the level of detail provided in the suggested references.

Modification:

Proteomics analysis

The new bone tissues of three specimens from each group were carefully separated right after sacrifice and immediately frozen by liquid nitrogen. After thorough grinding, the phenol extraction method was applied for protein extraction. Specifically, phenol extract was prepared by adding 2.4 g sucrose, 0.058 g NaCl, 0.146 g EDTA·2Na, 0.02 g DTT, 2.5 mL 0.5 M Tris-HCl (pH 6.8), 2.5 mL 1.5 M Tris-HCl (pH 8.8) and adjusting the volume with ddH_2O to 10 mL. Then an equal volume of phenol-Tris-HCl (pH 7.8) saturated solution was added and mixed at 4°C for 40 minutes. After collection of the upper phenol phase through centrifugation, five times the volume of pre-chilled 0.1 M ammonium acetate-methanol solution was added and precipitated for 24h at -40°C. Precipitates were then collected and washed with pre-chilled methanol and acetone, respectively. Then precipitates were dissolved in lysis buffer at room temperature for 3-5 minutes. Centrifuge the solution to collect the supernatant, which is the total protein

solution of the sample.

Western blot assay

Proteins (30 μg /lane) were separated using the same methods as the proteomics test.

17. 87-88"The TMS, however, exhibits its distinctive two-stage behavior." explain using the collected data exactly what the behaviour is.

Response: Thank you for this comment. We have now provided a more detailed explanation of the two-stage behavior of the TMS here. And the quantitative explaination of the mechanical behavior is described later at the magnification of the strain-stress curve in Fig. 2d.

Modification: The TMS, however, exhibits its distinctive two-stage behavior: at the initial stage with strain less than 2.5%, the compressive stress is relatively inconspicuous, while a more significant increase in stress occurs after larger strains are applied (Fig. 2c). To quantitatively describe the compression deformation process, Fig.2d depicts the magnification of the strain-stress curve within the maximum threshold of strain that promotes bone formation (5%).

18. 92-93 in your materials and methods you mention that 60 N is twice the weight of the average rabbit. However, previously you describe the primary stress conditions as 1/6th of the weight of a rabbit. 1/6th of 30 N is 5 N instead of 10 N (10 N would be 1/3rd of the rabbits weight). Please clarify which is correct, also correct the results and conclusion section accordingly.

Response: Thank you for pointing this out. We have reviewed the manuscript and clarified the discrepancy regarding the primary stress conditions. The correct value should be 1/3rd of the average rabbit's weight, which is approximately 10 N.

Modification: This innovative design aims to decouple the modulus and strength of the scaffold. Specifically, under primary stress conditions (10N, 1/3 of the experimental animal's weight)

19.The graphical and data visualisations are of excellent quality. Please add the technical and biological replicates in the figure captions of all figures.

Response: Thank you for your kind feedback. We have added the information of replicates to the figure captions of all relevant figures in the manuscript.

20.An exception to this is in figure 4r and 4s. first there is no scale bar in figure 4r and there is no mention of what the size of the scale bar is in figure 4s. In the description of these figures the authors state "the collagen fiber appeared to be more random of CS. Whereas in the TMS, the collagen showed a pronounced orientation parallel to the loads." (line 222-223). This is not overly clear from the figures and more detail need to be given to support this statement. I can see from the orientation map there seems to be some improvement in orientation, but would it be possible to quantify this a bit more. For example, the authors can measure collagen alignment in the figures via the method given in this paper doi: 10.1007/978-1-4939-7113-8_28), which will provide a stronger argument for this observation.

Response: Thank you for your detailed observations and suggestions. We apologize the omission of the scale bar in Fig. 4r and the lack of the scale bar size, which was shown in Fig.S11. These details have now been added for clarity and consistency. Regarding the description of collagen fiber orientation, as outlined in the referenced paper (DOI: 10.1007/978-1-4939-7113-8_28), there are several open-source software tools available for this purpose. In our study, we used the OrientationJ software, which is also mentioned in the referenced article. The primary difference between OrientationJ and the CurveAlignment software in the referenced paper lies in the global measurement approach and computational load; Still, this diffence does not affect the actual calculation accuracy. In our analysis, we characterized collagen orientation for only four images, resulting in a manageable computational load. We have included the collagen alignment distribution in Fig. S11. To provide clarity, we have adjusted the scale factor for collagen orientation and added detailed descriptions of all software parameters used in the Methods section.

Modification:

OrientationJ was connected to a macro that carried out orientation analysis within several 10×10-pixel sub-ROIs that covered the overview image in a grid-like pattern with finite difference greadient method. The primary fiber orientation was visualized as a yellow line in each sub-ROI with a a scale factor of 150 % and diffrenciation energy (defined as the trace of the structure tensor matrix). The length of the line indicates the degree of anisotropy. Normalized energy and angles was also plotted to show the fiber orientation.

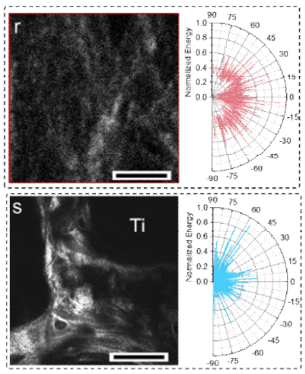

Fig. 4 Histomorphological evaluations of the critical defect healing. r, s SHG imaging and orientation map of collagen fiber at 4 weeks. Scale bars = 100 μm.

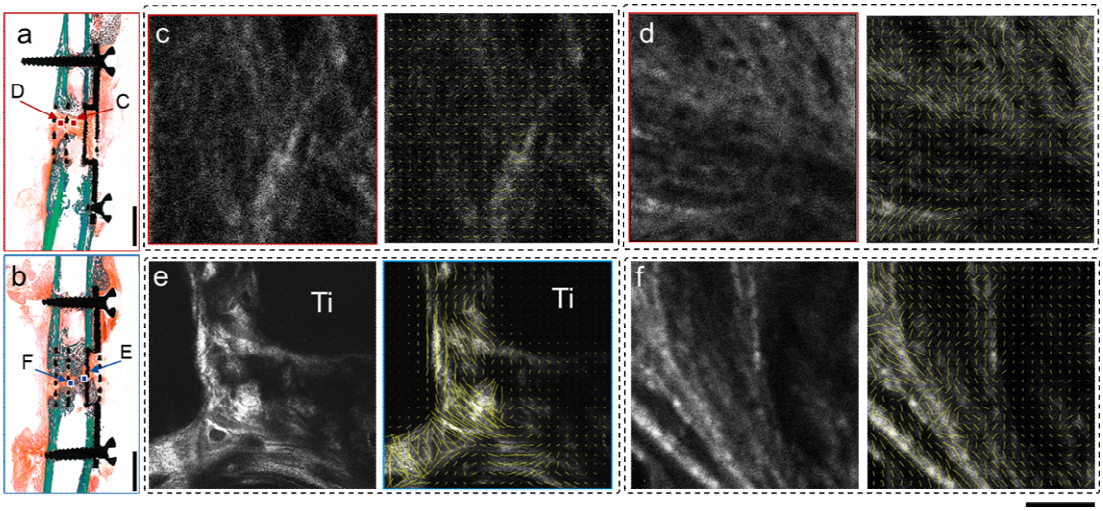

Fig. S11 SHG imaging of fiber orientation of bone tissues. a,b position of tested fiber orientation with implantation of CS and TMS. **c-d** Magnifications of label ROI with SHG imaging. The primary fiber orientation was visualized as a yellow line in each sub-ROI. The length of the line indicates the degree of anisotropy. Scale bars = 100 μm.

21. Line 237: "Subsequently, proteomic and Western Blotting (WB) were conducted" should be "Subsequently, proteomic analysis and Western Blotting (WB) were conducted"

Response: We sincerely thank you for the proofing. The text was modified accordingly.

Modification: Subsequently, proteomic analysis and Western Blotting (WB) were conducted

22. While you have correctly noted where there are areas of significant differences between samples, potential reasons must be given for where no significant differences were noted, which in the case of figure 3 appears to be between CS and TMS at 8 weeks (figure 3b), between any group at 8 weeks (3c) and between any groups (figure 3d).

Response: Thank you for this comment. Previously, we intended to mark significant differences only in groups where it was necessary to highlight findings, which did not imply the absence of significant differences in other groups. We agree with your suggestion and have marked all groups which have significant differences. Additionally, we have included a "Statistical analysis" section in the Methods to clarify this point and uploaded the source data for reference.

Modification:

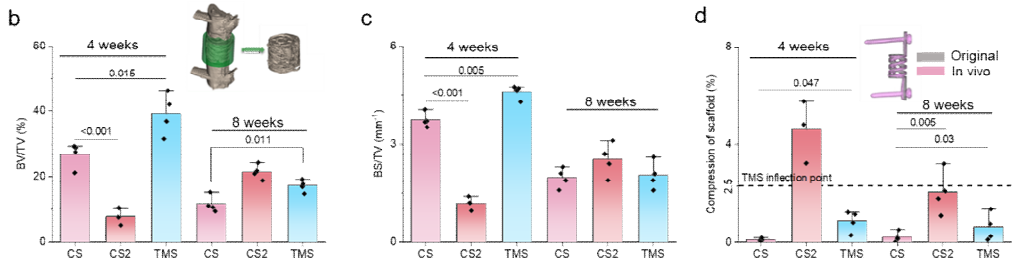

Fig. 3 TMS enhanced bone regeneration with proper tissue strain. b, c Osteogenesis in the green region of interest (ROI) was quantified by two indicators: bone volume/tissue volume (BV/TV) and bone surface area/ tissue volume (BS/TV). **d** In vivo compression of scaffold calculated from the original and post-implantation lengths.

Statistical analysis

The numerical data were analyzed using Origin 2019b (OriginLab, Northampton MA, USA), employing one-way analysis of variance (ANOVA) followed by Tukey's post hoc multiple comparison test. Data are presented as mean ± SD ($n \geq 3$, independent samples). Statistical significance was determined with p values.

23.Figure 5 is excellent, although figure 5f looks more like a graphical abstract or a figure that can be included in the intro to provide a pictorial overview of this study.

Response: Thank you for your positive feedback on Fig. 5. We appreciate your suggestion and combine Fig.5f to Fig.1 in the introduction section to better contextualize the study's scope.

Modification:

[figure redacted]

Fig. 1 Workflow of the proposed metamaterial scaffold. a Structural design of a two-stage metamaterial scaffold (TMS) for critical bone defects. **b** Electron-beam 3D printing technique fabricates the proposed metallic TMS and classic scaffold (CS) design. **c** Mechanical tests demonstrate the two-stage modulus of TMS. **d** Afterwards, scaffolds are in vivo implanted in

rabbits' critical ulnar defects, and TMS illustrates promotion of angiogenesis and osteogenesis.

24.Line 338: "for compress-dominated applications" should be "for compression-dominated applications"

Response: We thank you for the proofing. The text is modified.

Modification: Consequently, TMS may be more suitable for compression-dominated applications.

Reviewer #5 (Remarks to the Author):

I co-reviewed this manuscript with one of the reviewers who provided the listed reports. This is part of the Nature Communications initiative to facilitate training in peer review and to provide appropriate recognition for Early Career Researchers who co-review manuscripts.

Response: Thank you for your contribution and input.